Modeling the behavior of ethanol and BTEX in groundwater contaminated with ethanol-85

Pieter W.F. van der Zon

Student nr. 3021734

Supervisor: Dr. S.M. Hassanizadeh

Department of Hydrology

University Utrecht

Abstract

The increased usage of ethanol, both as a biofuel and as an oxygenate, has heightened concerns about the possible negative effects of ethanol on the environment. In this thesis several conceptual models are constructed to investigate the effects of a controlled release of 200L E85 (i.e. 85% ethanol and 15% gasoline by volume) in the unsaturated zone as part of field experiments carried out by the Federal University of Santa Catarina, Florianopolis, Brazil. Using temperature and rainfall data, the models were used to investigate the effects of water table oscillations on the spreading of E85. Results from the numerical simulations using the HYDRUS-1D software package indicate that without water table fluctuations, ethanol and BTEX are retained mostly in the unsaturated zone. In agreement with experimental data by Schneider (2012), model predictions further indicate that water table oscillations cause ethanol to migrate to greater depths in the saturated zone. A sensitivity analysis is carried out to investigate the effects of several physical and chemical parameters on the transport calculations, as well as the presence of a plastic cover placed on top of the field site. Suggestions for future numerical studies are given also.

Table of contents

1. Introduction

Anthropogenic contamination of soil and groundwater resources by gasoline or oil is a major concern nowadays. Increasing attention on this topic has led to numerous research projects investigating the effects of gasoline spills on the environment, both on local and global scales. During the last decade several of these projects considered the environmental effects of oxygenates such as methyl tert-butyl ether (MTBE), ethanol and methanol. Although oxygenates may be beneficial in terms of improving air quality (e.g. Niven [2005]), concerns are increasing about the possible negative effects of oxygenates on groundwater quality (Poulsen et al. [1992], Powers et al., [2001], Niven [2005]). Possible adverse health effects regarding MTBE have stimulated much research, especially after implementation in 1990 of the Clean Air Act in the USA. This law required the phasing out of MTBE as a fuel oxygenate by 2005 and its replacement by ethanol (Österreicher-Cunha et al., [2009]).

In Brazil, ethanol-blended gasolines (i.e. gasolines using ethanol as an oxygenate) have been used for over 30 years, in part spurred by governmental subsidies for this type of fuel. However, also in Brazil concerns have arisen about the possible impacts of ethanol blended gasolines on soil and groundwater resources.

The more extensive use of ethanol as an oxygenate is likely to lead to its more frequent encounter in groundwater plumes containing BTEX (benzene, toluene, ethylbenzene, and xylene). However, a considerable hiatus exists in available information on ethanol since, especially during the 80's and part of the 90's, ethanol was not viewed as a pollutant. Furthermore, misconceptions existed that no important differences existed between the ethanol-blended and standard blend gasolines (Powers et al. [2001]).

Both laboratory-scale and field-scale experiments have been conducted over the years to study the fate and transport of gasoline, ethanol and gasoline/ethanol mixtures in soils and groundwater (e.g., Heerman and Powers [1998], McDowel and Powers [2003], Corseuil et al. [2004], Freitas and Barker [2011]). Field conditions are generally different from laboratory measurements because of soil heterogeneity, transient weather conditions and water table fluctuations. In order to obtain more insight into the effects of gasoline/ethanol mixtures on groundwater contamination, field experiments were recently set up at the Ressacada experimental farm of the Federal University of Santa Catarina (UFSC) in Florianópolis, SC, Brazil. The experiments were part of collaboration since 1995 between UFSC and Petrobrás, the Brazilian oil company, to study the interactions of ethanol and gasoline (Corseuil et al. [1998]). The gasoline/ethanol field studies at the Ressacada farm are

controlled release experiments in which the subsurface transport of small spills of fuels commonly used in Brazil are studied. This includes studies of biodiesel, E20, and E85, where E stands for ethanol and the corresponding number represents the percentage of ethanol in the gasoline.

Many studies considering ethanol have been focusing mainly on the the saturated part of subsurface systems (e.g. Corseuil et al [2004], Zhang et al. [2006], Gomez et al. [2009]). However, there are numerous processes that affect the ultimate concentration of chemicals in groundwater, including infiltration of the gasoline into the unsaturated zone of the subsurface (Powers et al. [2001]), and sorption/desorption and volatilization processes.

While several recent studies have shown interesting results regarding the fate and transport of ethanol in the unsaturated zone (McDowell [2003], Österreicher-Cunha et al. [2009]), few investigated E85 or considered the release of only very small quantities of gasoline. The purpose of this thesis is to investigate the effects of a controlled spill involving 200L of E85 (85% ethanol, 15% gasoline (by volume) in the unsaturated zone of the Ressacada experimental farm of UFSC. Results of the field experiments will be analyzed in terms of a one-dimensional conceptual model developed for the unsaturated zone based on the Hydrus-1D computer software package (Šimunek et al. [2008]). Modeling results will be compared with results from other studies, including small-scale sandbox experiment carried out by McDowell and Powers [2003]

Österreicher-Cunha et al. [2009] previously showed that ethanol in the spilled gasohol quickly partitions into residual water in the vadose zone and is retained there as the gasoline continues to infiltrate. For the conditions tested by McDowell and Powers [2003], over 99% of the ethanol was initially retained in the vadose zone. However, early results from the E85 field experiment (Schneider, 2012) suggested that ethanol and BTEX both reach the saturated zone (or at least the capillary fringe) relatively quickly after their release.

The contradictory results may have to do with the transfer processes that are occurring. On the one hand, there is the transfer of ethanol to the water phase (e.g. McDowell and Powers [2003]), while on the other hand water may transfer also to the ethanol (current experiment). The size of the spill may also influence the transfer process, as well as the presence of multiphase flow (which will not be considered here). The Hydrus-1D approach will be used here to analyze as best as possible some the data of the Ressacada field experiment so as to obtain more insight in the processes taking place in the subsurface. In particular the question will be addresses if the ethanol plume of the controlled release experiment can be quantified with a 1D model for the unsaturated zone and if the modelling results are consistent with the Ressacada field data.

2. Literature Review

In this chapter a brief overview is given of various physical and especially chemical processes that may affect ethanol transport in the vadose zone and groundwater. The focus is on the processes of cosolvency (section 2.1), sorption (section 2.2), volatilization (section 2.3) and the presence of ethanol in the capillary fringe (section 2.4).

2.1. Cosolvency

Ethanol has the potential to increase the concentration of BTEX species in groundwater [Powers et al., 2001]. This could lead to enhanced environmental pollution by increasing both length and longevity of plumes of fuel-contaminated groundwater due to spreading of hazardous components (e.g. benzene). Corseuil et al. [2004] studied the cosolvency effects of ethanol on the solubility of BTX compounds in water. Using a Brazilian commercial gasoline containing 22% ethanol and exposing the fuel to varying volume ratios of water, they achieved a maximum volume fraction of 15% for ethanol in the aqueous phase. They showed that an aqueous concentration of 10% ethanol increased BTX concentrations by 30%. The presence of alcohols furthermore increased the equilibrium concentrations of BTX depending upon the hydrophobicity of the component. For example, benzene had a smaller increase than xylene since it is less hydrophobic).

Using computer and laboratory experiments, Barker et al. [1991] concluded that methanol-85 in a gasoline pool at the water table quickly dissolved into the groundwater. High aqueous phase concentrations of BTEX were associated with the initial period of contamination due to cosolvency effects of the methanol, thus creating a slug of highly contaminated groundwater that was transported downgradient by advection. Once the methanol source was depleted from the gasoline, however, BTEX concentrations were also reduced.

2.2. Sorption

One removal process contributing to the natural attenuation of groundwater is sorption of hydrocarbons to soil material. Similar to the cosolvency effects described earlier, the presence of ethanol (or other cosolvents) will lead to increased groundwater concentrations (i.e. less sorption) due to the reduced polarity of the aqueous phase. Hence, the retardation of BTEX concentrations will be reduced in the presence of ethanol and transport rates may increase.

These effects of sorption were shown also by Rixey [1994] who used a 1D-model to demonstrate that when methanol cosolvent-dependent sorption was included, the BTEX components moved faster

through the porous medium. However, the author also noted that these effects would be significant only where aqueous methanol concentrations were larger than 10 to 13 weight percent.

2.3. Volatilization

Volatilization may contribute to the removal of contaminants from a soil. For example, Österreicher-Cunha et al. [2009] investigated the effect of ethanol on the behaviour of gasoline in an unsaturated tropical soil. They report the importance of both ethanol and water content in the process of volatilization. For standard gasoline, a larger water content may, up to a certain point, lead to increased volatilization as the water does not allow contact between gasoline and soil particles. When ethanol is blended with gasoline, the cosolvency effect of ethanol on the BTEX compounds modifies water characteristics as the water becomes laden with BTEX. Hence, the remaining unsolubilised gasoline-ethanol may volatilise more easily, as more BTEX are retained in soil water (Österreicher-Cunha et al. [2009]). Furthermore, the authors mentioned that ethanol addition to gasoline can increase its vapour pressure, with a maximum increase for a 10% v/v mixture. However, for high ethanol blends this effect was found to be negligible. Nonetheless, other studies with sandy soils and ethanol-blended gasoline (e.g. Dakhel et al. [2003]) have shown that volatilisation can be responsible for more carbon removal than biodegradation of gasoline compounds (including BTEX) in an unsaturated soil, while biodegradation seemed to be the main process involved in disappearance of ethanol under the assumption that the dissolved and gaseous phases obey Henry's law (Österreicher-Cunha et al. [2009]).

2.4. Effects of ethanol on the capillary fringe

When released in a soil, ethanol can have a profound effect on the capillary fringe. McDowell et al. [2003] showed in a no flow tank that E95 was transported to the capillary fringe, and that an ethanol-induced reduction in the surface tension caused a significant collapse in the height of the capillary fringe. Stafford et al. [2007] demonstrated in a sand tank experiment that a released E95 blend tended to move to the top of the capillary fringe and spread longitudinally, which may lead to higher contaminant concentrations and more horizontal spreading (Stafford et al. [2011]). This may partially be the effect of the buoyancy of ethanol, which causes it to remain above the water table into the partially collapsed capillary fringe (Stafford et al. [2007]).

3. The Ressacada Field Site

In this chapter a description is given of the Ressacada field site Federal University of Santa Catarina in Florianopolis, along with pertinent information for soil, hydrogeologic and meteorologic characterization of the site.

3.1. Site description

The area of the E85 controlled release experiment is located at Fazenda Experimental da Ressacada (the Ressacada Experimental Farm), located south of the city Florianópolis, in the region of Tapera near the airport of Hercílio Luz, Brazil. The field site comprised an area of approximately 105 m^2 (13 m long and 8 meter wide). A small trench (1.0 m long x 1.5 m wide x 0.20 m deep) was excavated for application of the ethanol/gasoline contaminant (figure 1). In total 200 L of E85 was applied. The location of the source of contamination is indicated by point F in figure 2. A large number of monitoring wells (36) had been installed in the direction of groundwater flow in order to monitor possible mass flow of the released E85 pulse (Figure 2). Each of the wells contained probes installed at depths of 0,6; 0,9; 1,2; 1,5; 2,0; 3,0; 4,0; 5,0 and 6,0 m, corresponding to different regions of the soil.

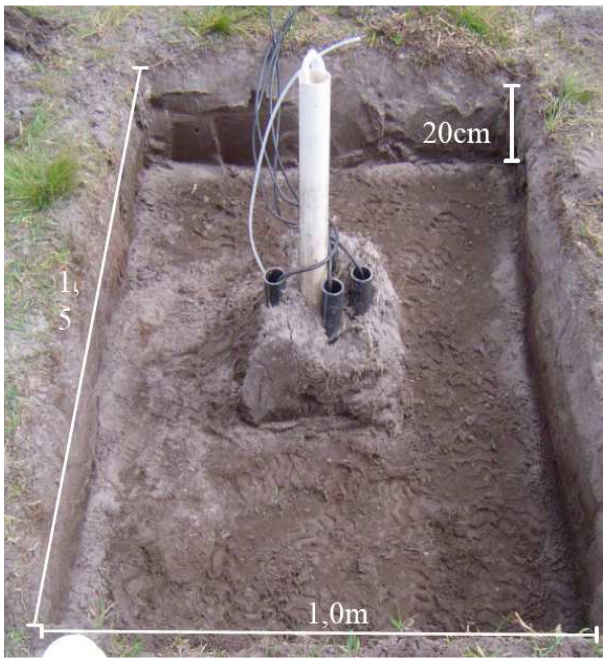

Figure 1: Area of release of the E85 experiment (picture taken from Schneider, 2012)

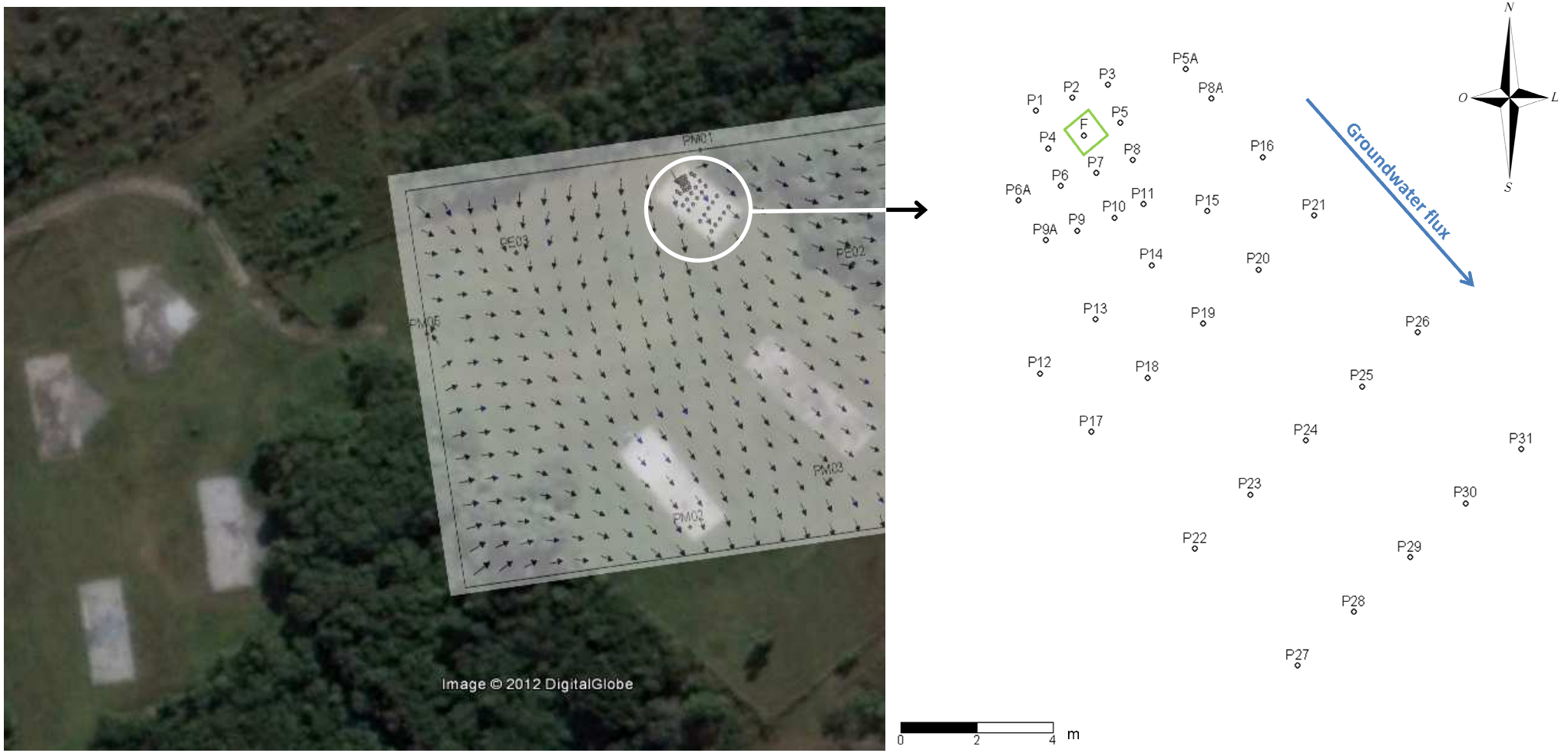
PM01
PE03
PE02
PM05
PM03
PM02
Image © 2012 DigitalGlobe
P5A
P3
P2
P8A
P1
P5
F
P4
P8
P16
P7
P6
P6A
P11
P15
P21
P10
P9
P9A
P14
P20
P13
P19
P26
P12
P18
P25
P17
P24
P31
P23
P30
P22
P29
P28
P27
Groundwater flux
N
O
L
S
0
2
4
m

3.2. Hydrogeological characterization

Florianopolis is an area having an average relative humidity of approximately 80%, with relatively high rates of precipitation in January and February, and much lower rates from April to June. Average temperatures in Florianopolis are approximately 24°C in the summer, and 17°C during winter. Precipitation and temperature data for the period 1-1-2010 until 31-07-2011 as used in this study were obtained from INMET, the Brazilian Meteorological Institute (Brasilia, DF, Brazil) (figure 3). Groundwater flow at the site occurs in different directions because of the presence of surface water and drainage areas that serve as a discharge area of the regional aquifer [Lage, 2005]. Figure 4 shows general flow directions as indicated by the blue arrows. The average groundwater velocity is between 5.2 and 6.2 m per year. Groundwater levels in the experimental area range from 0.7 m to a depth of 1.6 m.

The controlled release of E85 was carried out on the 9th of September, 2010. A total of 200 liters of the ethanol-gasoline mixture was applied, corresponding to a net spill of 170 liters of ethanol and 30 liters of gasoline. After releasing the E85, the area was covered with water-repelling plastic and a small layer of gravel on top to prevent precipitation from directly entering the soil at the experimental site. A schematic cross-section of the source zone is given in figure 5.

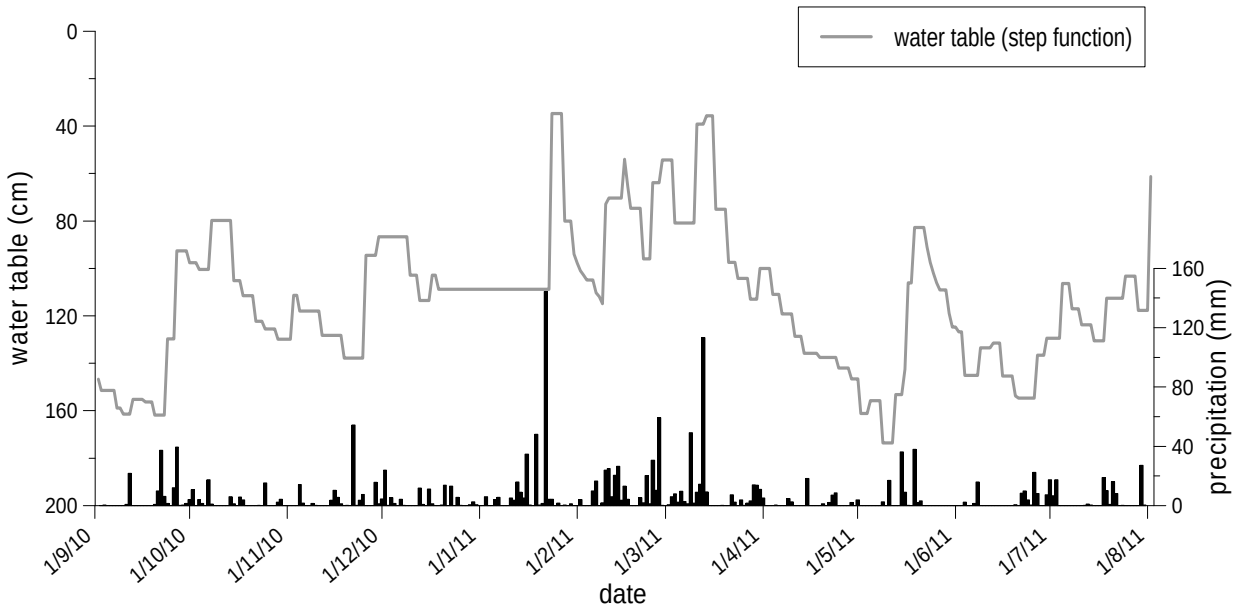

Figure 3: water table fluctuation and precipitation during the period of the simulation

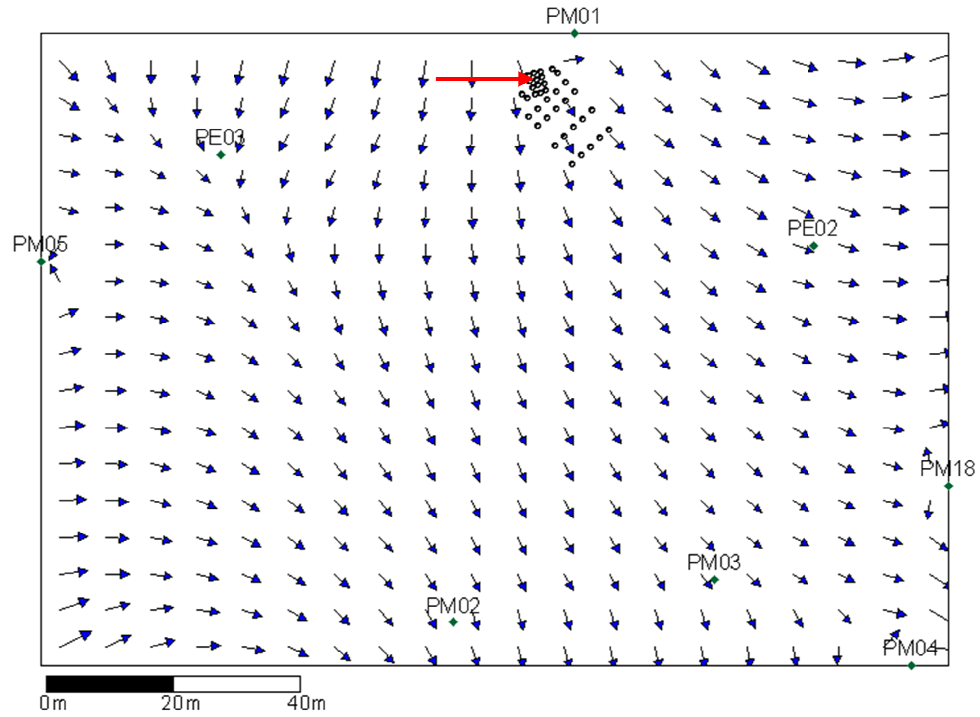

Figure 4. Groundwater flow directions at the Ressacada field site. The red arrow shows the area of release of the E85 mixture, while PM#'s indicate locations of the different piezometers.

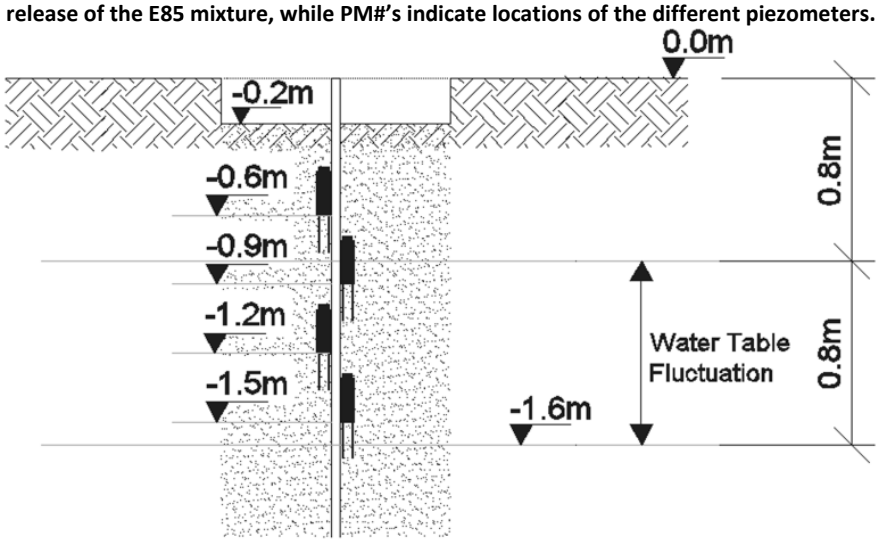

Figure 5. Schematic cross-section of the source zone. The displayed range of water table fluctuations was for the first 30 days E85 release (picture taken from Schneider and Corseuil [2012]).

In April 2010 a lithological profile of the E85 experimental area was taken by the team of Prof. Dr. Chang Hung Kiang, Department of Applied Geology of the Universidade Estadual Paulista (UNESP), Rio Claro, São Paulo, Brazil. The geophysical survey was carried out by means of an electrical resistivity method (GPR), which consists of introducing an electric current into the ground. The induced method uses electromagnetic radiation in the microwave band (UHF/VHF frequencies) of the radio spectrum, and detects reflected signals from subsurface structures to calculate the resistivity of geological materials.

Using this survey, resistivity values between 500 and 2000 Ω·m were obtained for the area of the E85 experiment. These values indicate that the soil can be classified as a sandy medium. (GL Technologies [1980]). Higher resistivity values (1000 to 2000 Ω·m) refer to coarse-textured sediments with elevated granulometry (larger grain size), while values less than 1000 Ω·m refer to sediments with a smaller grain size or sediments with a more fine-textured matrix. Findings of the geophysical survey are presented in Annex 1. Note that below 1.5 m, resistivity values decreased since the sediments at this depth were fully saturated at the time of the measurements.

The resistivity values given above are in agreement with soil samples from the Ressacada experimental area. Soil analyses were carried out by the Laboratório de Mecânica dos Solos (Soil Mechanics Laboratory) of the Federal University of Santa Catarina (UFSC), and are given in Figure 6. With 5.76% clay and 4.15% silt, according to the soil textural triangle (Figure 7), the soil classifies as a sand.

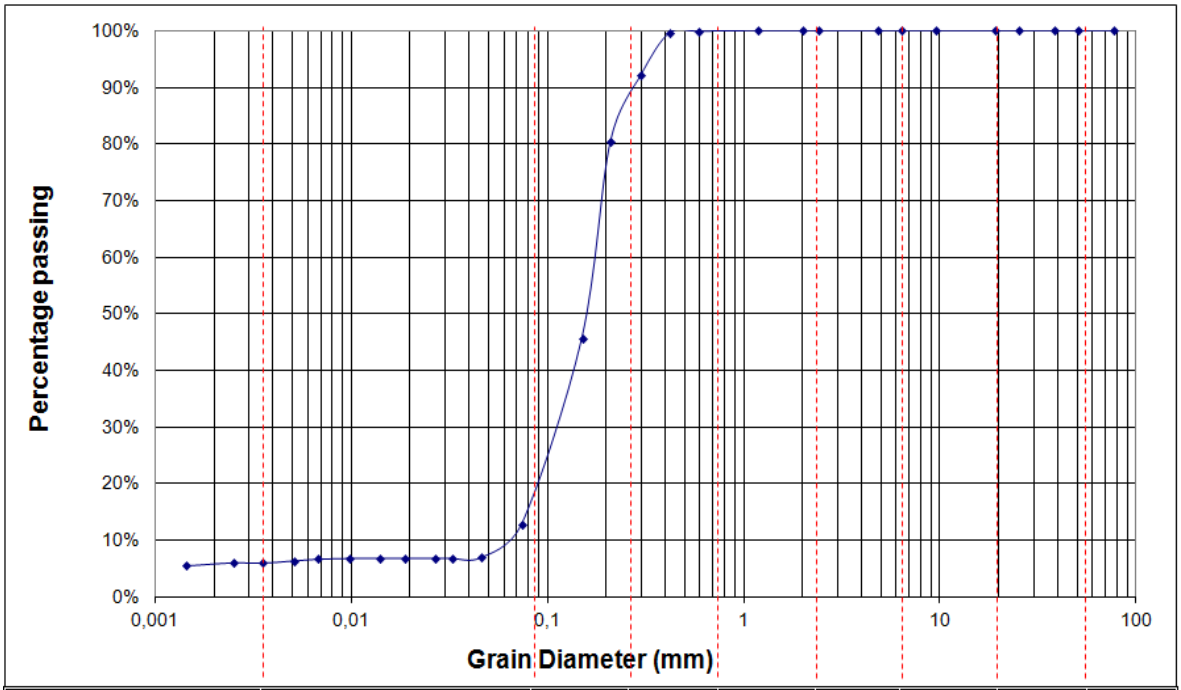

Clay	Silt	Fine Sand	Medium Sand	Coarse Sand	Fine gravel	Medium Gravel	Coarse Gravel	Boulder
5,76%	4,15%	70,62%	19,39%	0,09%	0,00%	0,00%	0,00%	0,00%

Figure 6: Grain size distribution

TDR (Time-Domain Reflectometry) was used to determine moisture contents in the field. TDR has the ability to accurately determine the permittivity (dielectric constant) of a material from the wave propagation due to the fact that there is a strong relationship between the permittivity of the material and its water content. During the E85 experiment, the dielectric constant was measured using a TRIME-IT,-ITC,-EZ,-EZC sensor (Schneider, 2012).

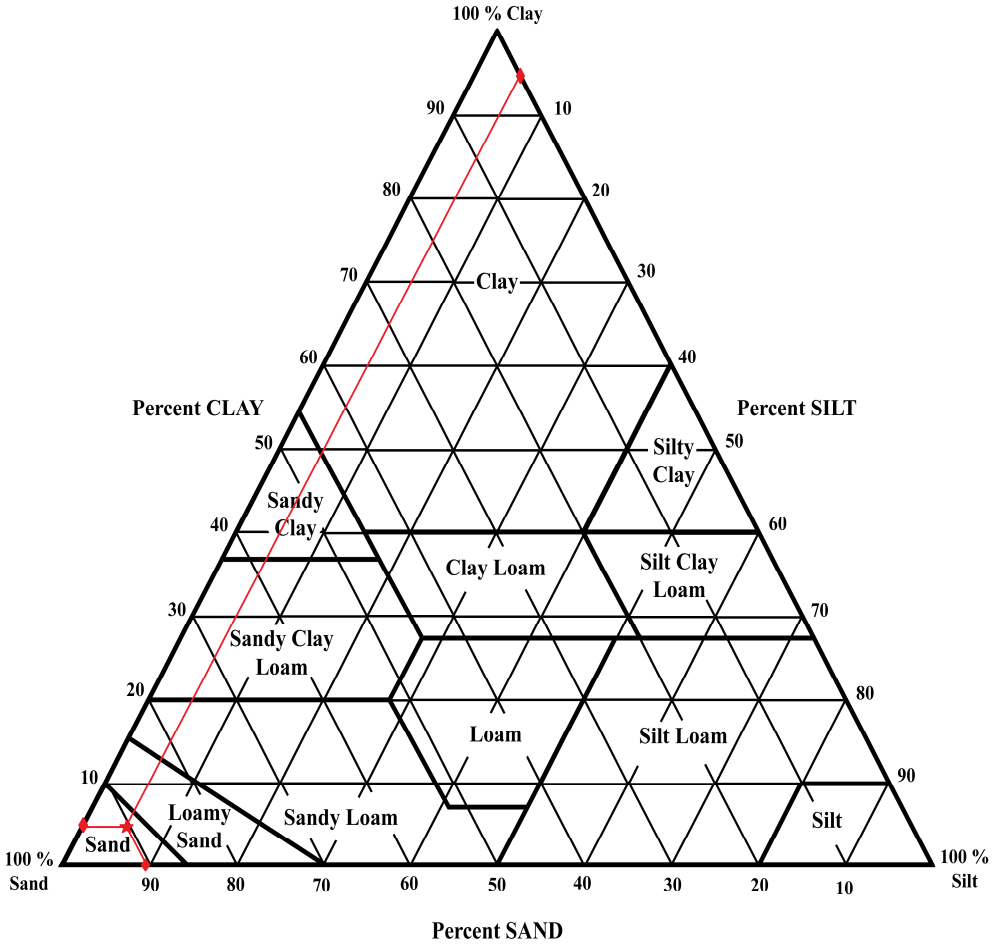

Figure 7: Soil textural triangle. Soil composition is at the intersect of the 3 lines.

Conversion from the measured dielectric constants to soil moisture content can be done using the equation of Topp et al. [1980]. With the results of their investigations of soil water content measurement using TDR, a calibration function was obtained (3rd order polynomial) given by:

$$\varepsilon_r = 3{,}03 + 9{,}3\theta + 146\theta^2 - 76{,}6\theta^3 \qquad (1)$$

where ε_r is the dielectric constant [-],and θ the volumetric soil water content [L L^{-3}]. Based on this relation and on the soil sample analyses Schneider [2012] developed an equation (equation 2) relating water content to ε_r. Figure 8 shows a plot of such a typical relationship, applicable to mineral soils [IMKO Micromodultechnik, 2006].

$$\theta = -0{,}98 + 1{,}897\varepsilon_r + 146\theta{\varepsilon_r}^2 - 76{,}6\theta{\varepsilon_r}^3 \qquad (2)$$

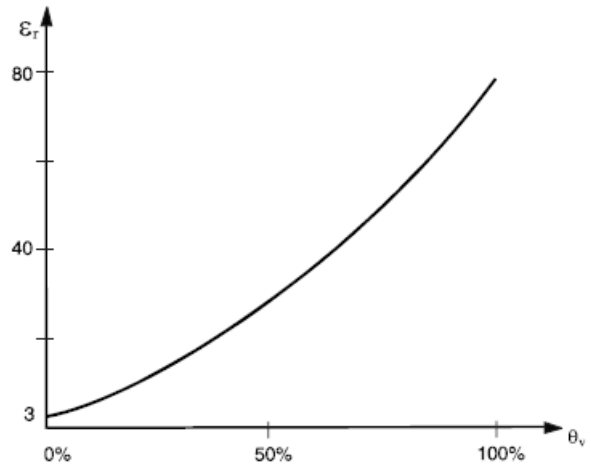

Figure 8. Relationship between the soil moisture content, θ (in vol. %) and the dielectric constant, ε_r.

3.3. Unsaturated Soil Hydraulic Properties

In this study the soil hydraulic properties needed for predicting water flow at the site are described using the constitutive relationships of van Genuchten [1980]. The soil water retention curve describing the relationship between the volumetric water content, θ [L L^{-3}] and the soil water pressure head, *h* [L], is given by:

$$\theta(h) = \theta_r + \frac{\theta_s - \theta_r}{[1 + (\alpha|h|)^n]^{1-1/m}} \tag{3}$$

where θ_r is the residual water content [L^3 L^{-3}], θ_s is the saturated water content [L^3 L^{-3}], α (>0, [L^{-1}]) is related to the inverse of the air entry pressure head, and *n* (>1 [-]) is a measure of the pore-size distribution (van Genuchten [1980]). Combining equation 3 with the pore-size distribution model of Mualem [1976], yields the following closed-form expression for unsaturated hydraulic conductivity (van Genuchten [1980])

$$K(S_e) = K_0 S_e^I \{1 - \left[1 - S_e^{n(n-1)}\right]^{1-1/n}\}^2 \tag{4}$$

In which effective saturation, S_e, is computed as

$$S_e = \frac{\theta(h) - \theta_r}{\theta_s - \theta_r} \tag{5}$$

and K_s is the saturated hydraulic conductivity [L T^{-1}], while I [-] is an empirical tortuosity parameter that is generally assumed to be 0.5 (Mualem [1976]).

In this study pedotransfer functions are used to estimate the unknown hydraulic parameters in Equations (3) and (4) (i.e. θ_r, θ_s, α, n, and K_s) from available soil texture and related data. Pedotransfer functions (PTFs) are predictive functions of certain soil properties from information or data that are more easily measured and may be more readily available. In this case the hydraulic parameters are estimated from soil texture and the dry soil bulk density using the neural network based pedotransfer functions derived by Schaap et al. [1998] in their Rosetta model, and embedded in the HYDRUS-1D software. The Rosetta pedotransfer functions within HYDRUS-1D were calibrated on a data set containing 2134 samples for water retention and 1306 samples for K_s. Many of the soil data used for the calibration were coarse-textured, which is also the case for the soil in this research.

Using the soil data from figure 6 and a bulk density of 1.55 g cm^{-3} the soil hydraulic parameters as predicted by Rosetta are given in table 1. The predicted residual and saturated water contents agree closely with TDR measured water contents from the field experiment, which showed a range of values between 0.09 to 0.39.

θ_r ($cm^3\,cm^{-3}$)	θ_s ($cm^3\,cm^{-3}$)	α (cm^{-1})	n (1)	K_s (cm day^{-1})	I (-)
0.0523	0.378	0.0324	2.55	310.6	0.5

Table 1. van Genuchten soil hydraulic parameters as predicted with the Rosetta pedotransfer functions within HYDRUS-1D (Schaap et al. [1998]).

3.4. Potential evaporation

Potential evaporation rates at the experimental site were computed with the equation of Hargreaves [1975], which was selected for its simplicity and accessibility to the required data. The Hargreaves equation can be described by:

$$E_p = 0{,}0023 R_a (T_m + 17{,}8)\sqrt{\delta_T} \qquad (6)$$

where E_p is potential evaporation [e.g. LT^{-1} or J $m^{-2}s^{-1}$], R_a is extraterrestrial radiation [same units E_p], T_m is the daily mean air temperature, which is computed as the average of the minimum and maximum daily air temperatures [^oC], and δ_T is the difference between the maximum and minimum air temperatures of a given day [^oC]. The extraterrestrial radiation, R_a [J $m^{-2}s^{-1}$], in water equivalents, can be calculated as follows:

$$R_a = \frac{G_{sc}}{\pi} d_r \left(\omega_s \sin\varphi \sin\delta + \cos\varphi \cos\delta \sin\omega_s\right) \quad (7)$$

where G_{sc} is the solar constant [J $m^{-2}s^{-1}$ or LT^{-1}] (1360 W m^{-2} or 4,789 cm/d), φ is the site latitude [rad], ω_s is the sunset hour angle [rad], d_r is the relative distance between Earth and Sun [-], and δ is solar declination [rad]. The variables ω_s, d_r and δ can be calculated as follows:

$$\omega_s = \cos^{-1}(-\tan\varphi \tan\delta) \quad (8)$$

$$d_r = 1 + 0{,}033 \cos\left(\frac{2\pi}{365} J\right) \quad (9)$$

$$\delta = 0.409 \sin\left(\frac{2\pi}{365} J * 1{,}39\right) \quad (10)$$

where J is the number of the day in the year, or Julian day [-]. Hence, by knowing Julian day, the latitude of Florianópolis, and daily minimum and maximum temperatures, potential evaporation can be computed.

4. Numerical Model

The Hydrus-1D software package was selected to simulate the transport of ethanol and BTEX components to the water table. According to the authors the model is especially useful for predicting water and contaminant transport in the vadose zone, and for analyzing specific laboratory or field experiments involving water flow and/or solute transport. Here we used the HYDRUS-1D code to simulate the release of an E85 spill at a depth of 0.25 m in a 250 cm deep soil profile having initially a water table at a depth of 1.6 m (Figure 3). In this chapter the equations describing water flow and contaminant transport at the site will be given (section 4.1), as well as applicable boundary conditions (section 4.2) and initial conditions (section 4.3).

4.1. Governing flow and transport equations

Water flow and solute transport processes at the site are described using the relatively standard Richards equation for variably-saturated flow, and the advection-dispersion equation for solute transport. Using the assumptions that the air phase plays an insignificant role in the liquid flow process and that water flow due to thermal gradients can be neglected, the Richards equation is given by ([Simunek et al. 2008]):

$$\frac{\partial \theta}{\partial t} = \frac{\partial}{\partial z}\left[K\left(\frac{\partial h}{\partial z} + 1\right)\right] \tag{11}$$

where, as before, h is the water pressure head [L], θ is the volumetric water content [L^3L^{-3}], t is time [T], z is the spatial coordinate [L] (positive upward), and K is the unsaturated hydraulic conductivity function [LT^{-1}]. The Richards equation will be used here assuming a one-dimensional partially saturated rigid, homogeneous soil profile.

The water retention, $\theta(h)$, and unsaturated hydraulic conductivity, $K(h)$, properties in the Richards equation can be described using a variety of single-porosity and dual-porosity functions (Simunek et al., 2008), such as the functions by Brooks and Corey (1964), van Genuchten (1980), Durner (1994) and Kosugi (1996). For this study, the van Genuchten-Mualem functions were selected as described in section 3.3).

Solute transport in a one-dimensional variably-saturated soil profile is assumed to be described by the following equation

$$\frac{\partial(\theta C)}{\partial t} + \frac{\partial(\rho_b s)}{\partial t} + \frac{\partial(ag)}{\partial t} = \frac{\partial}{\partial z}\left(\theta D^w \frac{\partial C}{\partial z}\right) + \frac{\partial}{\partial z}\left(aD^g \frac{\partial g}{\partial z}\right) - \frac{\partial qC}{\partial z} \tag{12}$$

where C is the solution concentration [ML^{-3}], s is the adsorbed concentration associated with the solid phase [MM^{-1}],g is the concentration of the gaseous phase, ρ_b is the soil bulk density [ML^{-3}], a is the air content [L^3L^{-3}], D^w and D^g are the dispersion coefficients [L^2T^{-1}] in the water and gas phases, respectively, and q is the volumetric flux (or Darcy-Buckingham velocity) [LT^{-1}]. Equation (12) assumes that any solute degradation can be neglected over the time periods considered in this study. If the solute is non-volatile, Equation (12) can be simplified by removing the terms accounting for accumulation in the air phase (i.e. g=0) and diffusion in the air phase. The governing transport equation then reduces to

$$\frac{\partial(\theta C)}{\partial t} + \frac{\partial(\rho_b s)}{\partial t} = \frac{\partial}{\partial z}\left(\theta D \frac{\partial C}{\partial z}\right) - \frac{\partial qC}{\partial z} \tag{13}$$

where D is now used for the dispersion coefficient. Equations (12) and (13) can be simplified further if one assumed linear equilibrium partitioning of the solute between the liquid and solid phases (i.e., applicability of a linear sorption isotherm between s and c):

$$s = K_d C \tag{14}$$

where K_d is distribution coefficient of the solute being considered[L^3 M^{-1}].

4.2. Boundary conditions

Solutions of the Richards equation for flow (equation 11) and the advection-dispersion equation for transport (equation 12) require knowledge of applicable boundary conditions at both the soil surface (*x*=*L*) and at the bottom of the assumed soil profile (*x*=0). For variably-saturated water flow a general flux condition is implemented at the soil surface (*z*=*L*) of the form

$$-K\left(\frac{\partial h}{\partial z}+\ 1\right)=q_0(t)\quad \text{at}\ z=L \tag{15}$$

where q_0 [LT^{-1}] is the prescribed potential soil water flux (Simunek et al. [2008]). Because the soil surface at the experimental site was covered by plastic immediately after release of the E85 mixture, q_0 in Equation (15) will be zero (leading to a second type or Neumann). However, also investigated in this thesis is the case where atmospheric boundary conditions apply to the soil surface. The flux $q_0(t)$ is then a function of time as defined by local weather conditions (precipitation and potential evaporation rates), but modified for possible system-dependent processes that allow for surface runoff when the soil cannot accept all rainfall, or when the soil is unable to provide all water as described by the potential evaporation rate (i.e., the evaporation rate decreases when the soil near the surface becomes very dry). These conditions are described in great detail in the HYDRUS-1D manual (Simunek et al., 2008).

A general boundary conditions for water flow that may be applied to the bottom of the soil profile is as follows

$$h(z,t)=\ h_0(t)\quad \text{at}\, z=0 \tag{16}$$

where h_0 [L] is the prescribed pressure head at a function of time, t [T]. In this study alternative conditions are considered: either a constant water table at some level below the soil surface (in which case h_0 is constant and defined by the height of water table above the lower boundary), or a variable water table boundary condition (in which h_0 has values consistent with observed water table data versus time; see figure 3).

In Hydrus-1D several types of boundary conditions (Dirichlet, Cauchy, Neumann) can be selected also for the solute transport equation. Assuming a non-volatile chemical, the appropriate boundary condition at the soil surface is

$$-\theta D\frac{\partial C}{\partial z}+qC=0 \quad \text{at } z=L \tag{17}$$

This condition presumes that no solute will cross the soil surface, either when the soil surface is covered by plastic (in which case q is also zero at the soil surface), or when transient atmospheric boundary conditions are used (thus assuming that rain or evaporating water contains no solutes). However, when a volatile chemical is present (such as the BTEX compounds), an additional term in Equation (17) is needed to account for gaseous diffusion from the soil through a stagnant boundary layer into the atmosphere. Following Jury et al. [1983], the modified boundary condition is of the form

$$-\theta D\frac{\partial C}{\partial z}+qC=\frac{D_g}{d}\left(k_g\,C-g_{atm}\right) \quad \text{at } z=L \tag{18}$$

where D_g is the molecular diffusion coefficient in the gas phase [L^2T^{-1}] and g_{atm} is the gas phase concentration in the atmosphere [ML^{-3}] above the stagnant boundary layer of thickness d [L] (Simunek et al. [2008]). In this study g_{atm} is set to zero. Equation (18) assumes that the volatilization flux is proportional to the difference in the air phase concentrations above and below the boundary layer.

The lower boundary condition for solute transport is set to be a zero-gradient condition of the form

$$\frac{\partial C}{\partial z}=0 \quad \text{at } z=0 \tag{14}$$

which permits solute to move downwards out of the system if there is also a water flux out of the soil profile. However, if the water flux is zero, the solute flux will also be zero.

4.3. Initial conditions

The initial condition for water flow in the soil profile is given by the general pressure head distribution

$$h(z,t)=h_i(z) \quad \text{at } t=t_0 \tag{20}$$

where h_i [L] is a prescribed function of z and t_0 is the time at which the simulation starts (i.e. the day of release of the E85 blend). The initial pressure head distribution was obtained by running a HYDRUS-1D simulation for one year using weather data from the Florianopolis region obtained from

the Brazilian weather institute INMET/SATMET. These data included measured precipitation data, as well as temperature data needed for calculating potential evaporation rates in the Florianopolis area. The pressure head distribution for the day of release (8 September 2010) was then selected to be the initial condition for the simulations (Annex 2), but modified to accommodate the volume of the E85 spill and an equivalent initial condition between depths of 25 and 55 cm. After adding the E85 ethanol/gasoline mixture, the excavated pit was immediately back-filled with the original soil material.

The initial condition for the solute was specified in terms of the total concentration, C_T, per unit porous bulk volume of the porous medium [ML^{-3}] given by

$$C_T = \theta C + \rho s + ag \tag{21}$$

where, as before, g as the gas phase concentration [$M\ L^{-3}$] and a is the air content [$L\ L^{-3}$]. Assuming linear equilibrium sorption onto the solid phase, and linear equilibrium partitioning between the liquid and air phases, Equation (21) reduces to:

$$C_T = (\theta + \rho K_d + ak_g)C \tag{22}$$

where k_g is an empirical constant [-] in Henry's law relating the solution and gas phase concentrations. Rearranging equation (22) gives the following equation for the solution concentration:

$$C = \frac{C_T}{\theta + \rho K_d + ak_g} \tag{23}$$

Hydrus-1D uses this equation to compute initial concentrations (at equilibrium) for the system for a given application of C_T over the specified depth of injection, which was taken to be 30 cm. Hence, C_T was implemented over the depth interval of 25-55 cm, which represented the spill as an equivalent initial condition. Concentrations of all solutes above and below this interval were set to zero. Values for the initial concentrations of ethanol and the BTEX compounds are given in table 2. Note that the total mass of BTEX released is based on their relative presence in the 30 liters of gasoline, and that they are not a substitute for the total 30 liters of gasoline, as can be induced from their total mass.

	Density [g/cm^3]	**Molecular weight** [g/mol]	**Henry's constant** [mg/L/mg/L]	**Diff Coef water** [cm^2/d]	**Diff Coef air** [cm^2/d]	**Mass released** [g]	K_{oc} [-]	K_d [cm^3/g]
Ethanol	0,79	46,1	0,00024	1,123	8813	134300	0	0
Benzene	0,88	78,1	0,23	0,864	7776	200	61,7	0,037
Toluene	0,867	92,1	0,27	0,795	6739	873	204	0,122
Ethylbenzene	0,867	106	0,32	0,734	5875	234	140	0,084
Xylenes	0,864	106	0,27	0,855	7344	1255	249	0,150

Table 2. Chemical parameter values used for ethanol and the BTEX compounds

5. Results and Discussion

Results of the HYDRUS-1D simulations are presented in this chapter. First results are given for the case of a constant water table (section 5.1), which is followed by the more realistic situation of having a variable water table as observed in the field (section 5.2). A brief discussion is provided next on how the results compare with previous studies (section 5.3).

Model parameters used in the HYDRUS-1D simulations are summarized in Tables 2 and 3. Please note that the distribution coefficient K_d for ethanol is zero (no sorption, and hence no retardation), while the BTEX compounds all are subject to some sorption, while also partitioning significantly into the gas phase as reflected by relatively high values of Henry's constant as compared to ethanol.

5.1. Constant water table

Since the water table is kept at a constant level at -158.8 cm during this time, and since the plastic on top of the soil is assumed to be impermeable to precipitation (and volatilization), ethanol is mainly transported downwards by diffusion after a very short initial phase involving some minor advective transport with redistributing source fluid (figure 9). Figure 10 shows distributions of ethanol with depth. Although ethanol is not subject to sorption (K_d=0) the chemical still remained nearly entirely in the unsaturated zone during the simulated period of 326 days.

Parameter	value	Source
Spill characteristics source zone		
Depth below ground surface [cm]	25	REMAS*
Depth area of release [cm]	30	REMAS
Width [cm]	100	REMAS
Length [cm]	150	REMAS
Area of release [cm^2]	15000	REMAS
E85 volume [L]	200	REMAS
Hydrogeology		
Saturated hydraulic conductivity [cm d^{-1}]	311	Rosetta
Saturated water content [-]	0,378	Rosetta
Residual water content [-]	0,052	Rosetta
α, parameter in soil water retention function [cm^{-1}]	0,032	Rosetta
n, parameter in soil water retention function [-]	2,55	Rosetta
I, tortuosity parameter in conductivity function [-]	0,5	Schaap et al. [1998]
Soil bulk density [g cm^{-3}]	1,55	
Longitudinal dispersivity [cm]	20	
f_{OC}, fraction of organic carbon	0,6%	Lage et al. [2008]
d, diffusion length at upper boundary [cm]	0,5	Jury et al. [1983]
General simulation		
Modeled area depth [cm]	250	
Simulation time [d]	326	

Table 3. Model parameters used for HYDRUS-1D simulations
(*measured at the Laboratório de Remediação de Águas Subterrâneas, REMAS, UFSC, Florianopolis, SC, Brazil)

Distributions of the BTEX compounds (fig. 11) are very different compared to those of ethanol. The BTEX compounds are redistributed much faster with depth and within 30 days after release are spread nearly equally with depth above the water table. However, when the BTEX compounds reach the capillary fringe at approximately 150 cm below ground surface, the rapid diffusion of the BTEX compounds essentially ends. These results show the importance of diffusion in the air phase for the BTEX compounds when no rainfall passes through the plastic and the unsaturated zone hence remains relatively dry. This is not surprising since diffusion coefficients in air are close to about 4 orders of magnitude larger than diffusion coefficients in water (Table 2). With increasing saturation near and below the water table, gaseous diffusion ceases and liquid phase diffusion becomes the main transport process. This is clearly reflected by the fact that the BTEX compounds do not move far below the water table. Their affective diffusion rates in the soil then become actually slightly less than the diffusion rate of ethanol because of sorption effects.

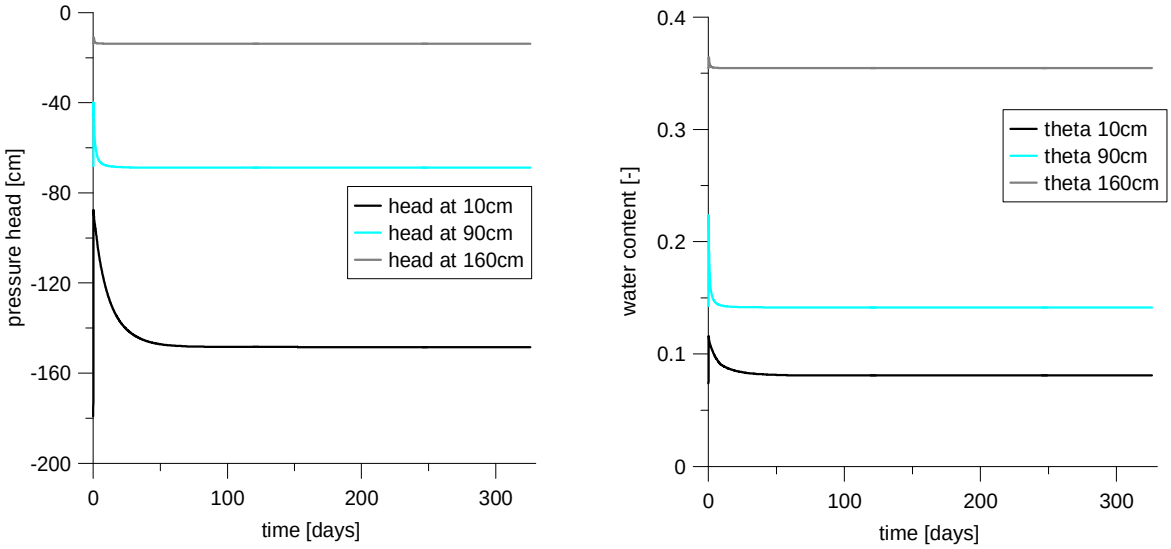

Figure 9: head and water content profiles at different depths

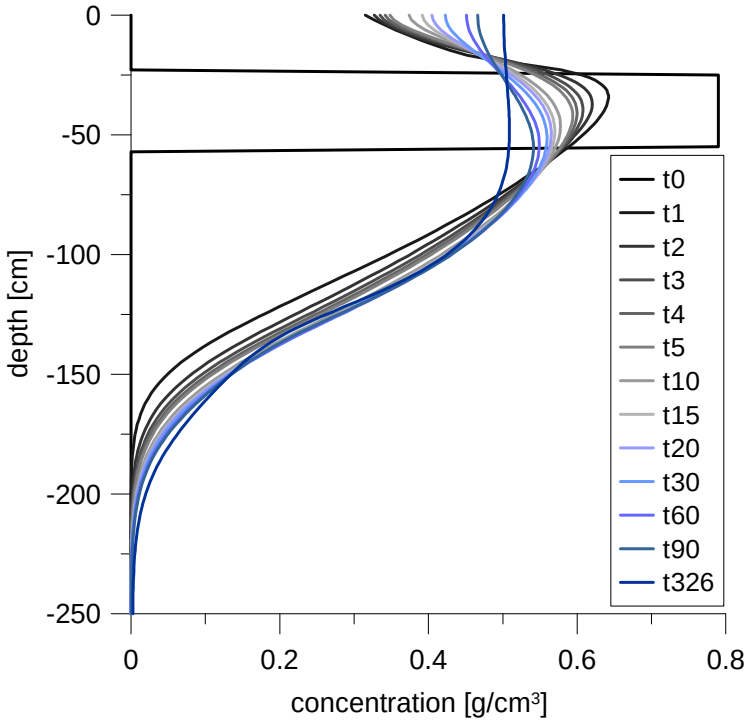

Figure 10: distributions of ethanol versus depth for the constant water table simulations.

Similar results are evident when considering calculated concentrations at numerical observation nodes located at different depths in the profile (figure 12). Observation nodes were placed in the unsaturated zone 90 cm below ground surface (bgs), just above the capillary fringe (145 cm bgs), and just below the water table (160 cm bgs). They show that maximum concentrations at 90cm bgs for the BTEX compounds are reached within 5 days after release of the E85 blend. For BTEX it can be seen that at higher saturations close to the capillary fringe and just below the water table,

concentrations increase at a slower rate than at 90cm depth. This effect is larger for toluene and the xylenes than for benzene and ethylbenzene.

Ethanol concentrations also increase rapidly at 90cm bgs, but similar trends can be observed at the other observation nodes, indicating that the distribution of ethanol stabilizes shortly after the release of E85. These results may be explained in part by the higher aqueous solubility of ethanol, but more likely due to the small value for Henry's constant, which is three or four orders of magnitude smaller than that for the BTEX compounds. Therefore ethanol is less likely to go into the air phase, leading to a much slower redistribution over depth. On the other hand, again, the larger effective diffusion coefficient of ethanol in water allows it to move more easily in the saturated conditions of the capillary fringe. Hence, once ethanol reaches the capillary fringe it is likely to move downwards at a faster rate than the BTEX compounds.

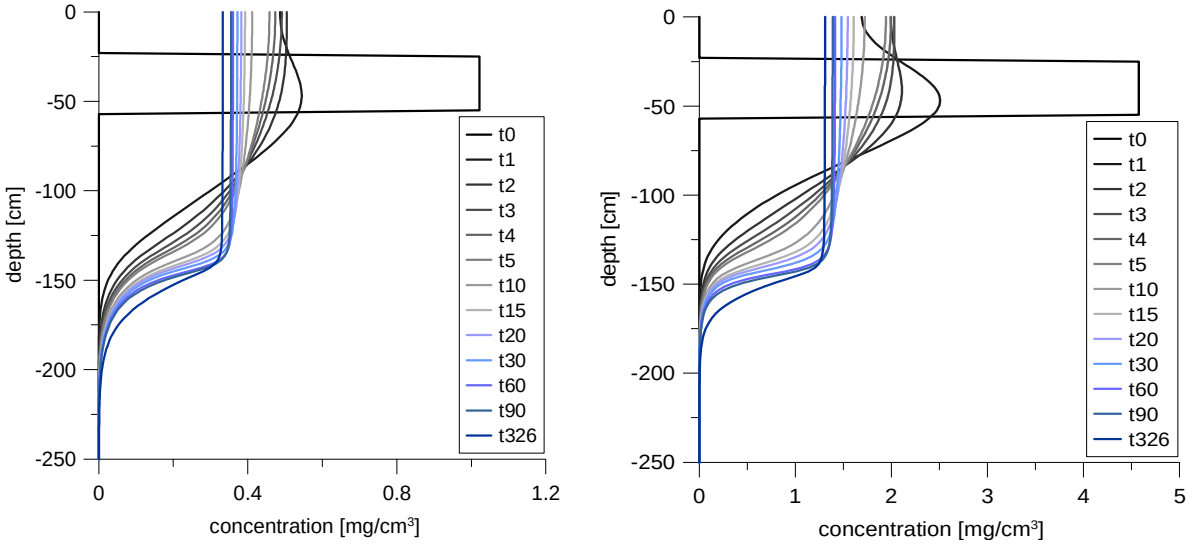

Figure 11: Distributions of benzene (left) and xylenes (right) versus depth for a constant water table

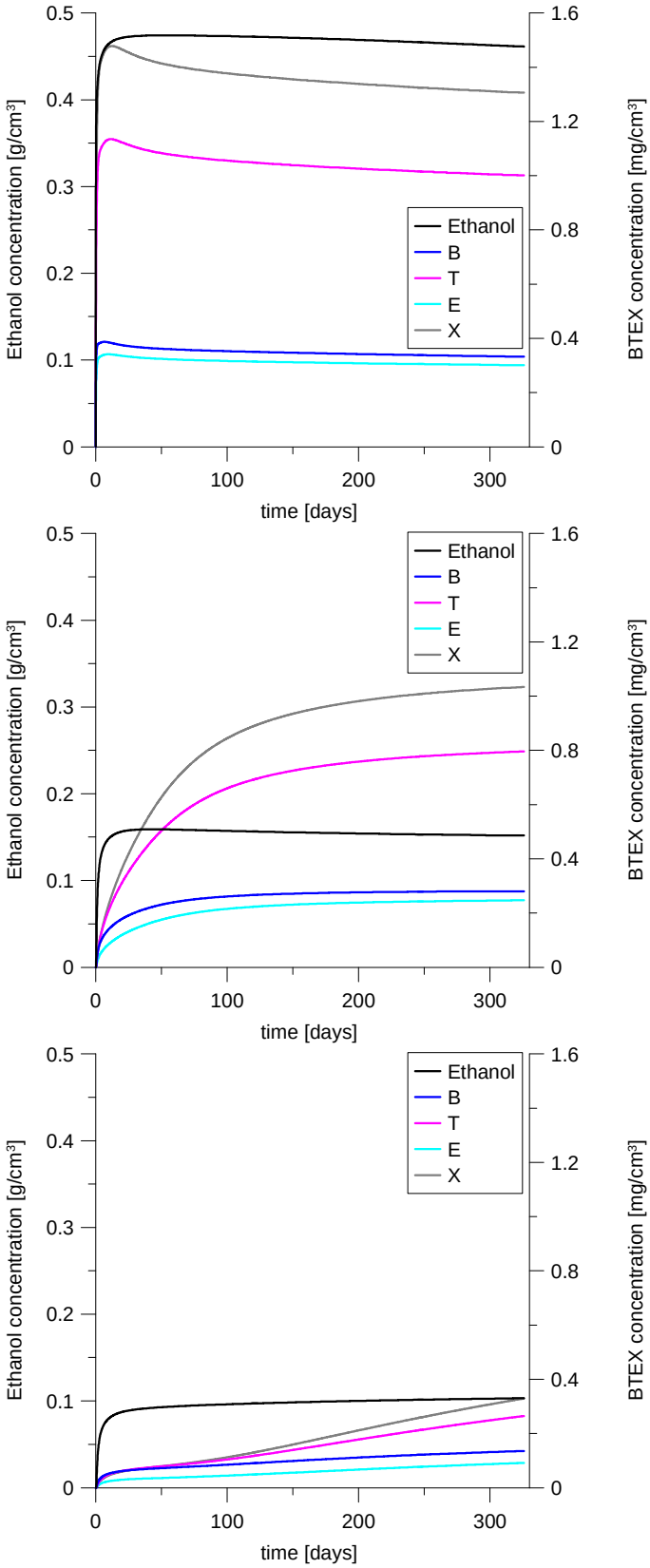

Figure 12: Ethanol and BTEX concentrations at 90 cm bgs (top), at 145 cm just above the capillary fringe (middle), and at 160 cm just below the water table (bottom)

5.2. Variable water table

In the case of a variable water table, results are quite different. The head profiles (figure 13) closely follow the movement of the water table (figure 3), with the profiles becoming smoother towards the surface. The first major water table rise occurred 13 days after release of the E85 mixture, causing the water content at the observation node of 90cm (figure 13) to move to saturation . Hence, for the first 13 days the ethanol and BTEX components should behave similarly as the constant water table scenario.

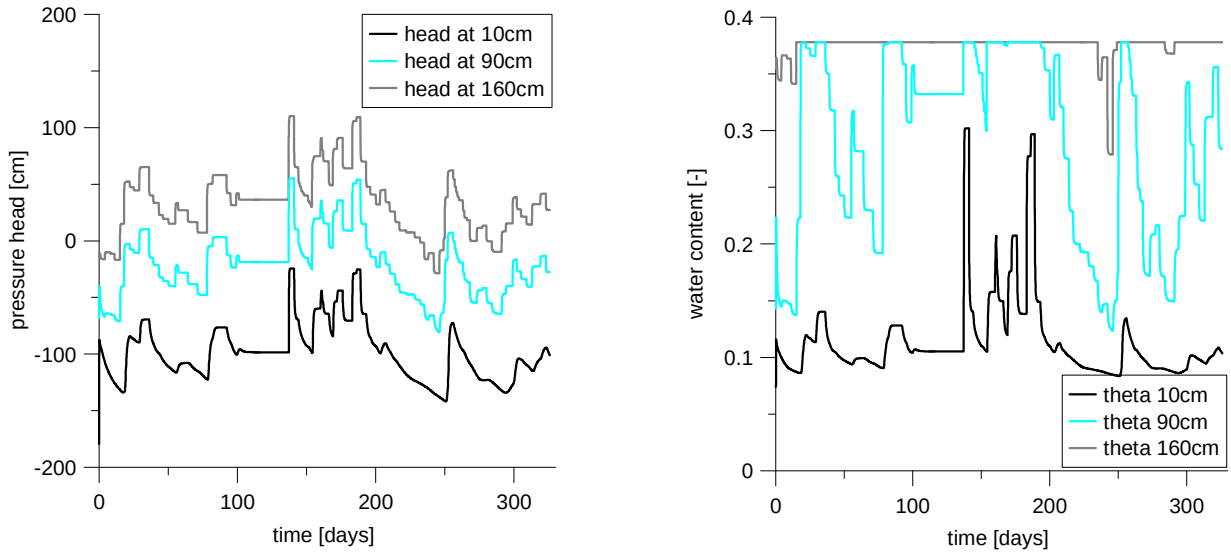

Figure 13: head and water content profiles at different depths for a variable water table

Comparing figures 9 and 14 shows that this is indeed the case, but after 20 days when the water table rises to approximately 80 cm bgs, most of the ethanol seems to move upward with respect to both the initial release and when a constant water table is present. This may be due to initial lack of mixing between the E85 and groundwater since, as time proceeds, ethanol spreads across the profile and reaches deeper into the system as compared to the simulation with a constant water table. At the end of the simulated period of 326 days, ethanol is now more equally spread across the profile.

Some of these effects may indeed be due to a lack of mixing when a step-function is used. When the water table increases more gradually, the E85 mixture has more time to move into groundwater while it rises. A step function does not account for this and may lead to a case where E85 is just simply pushed upwards by advection. The BTEX compounds show a similar trend as ethanol (figure 15), although at the time of the first major water table rise they have already penetrated deeper into the profile. Between 15-30 days only a minor fraction of the BTEX compounds reaches depths below the initial water table at 158.8cm.

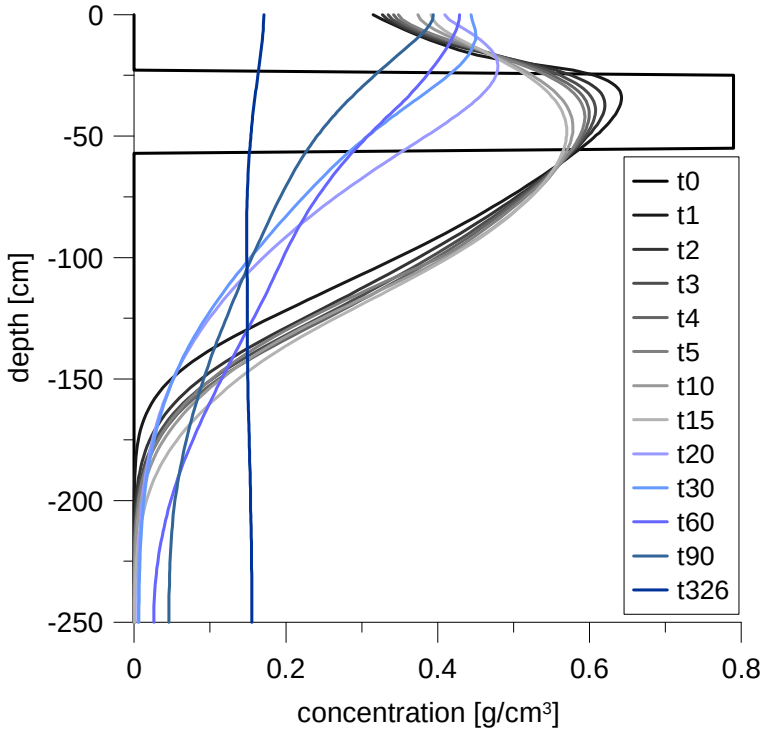

Figure 14. Distributions of ethanol versus depth with a variable water table

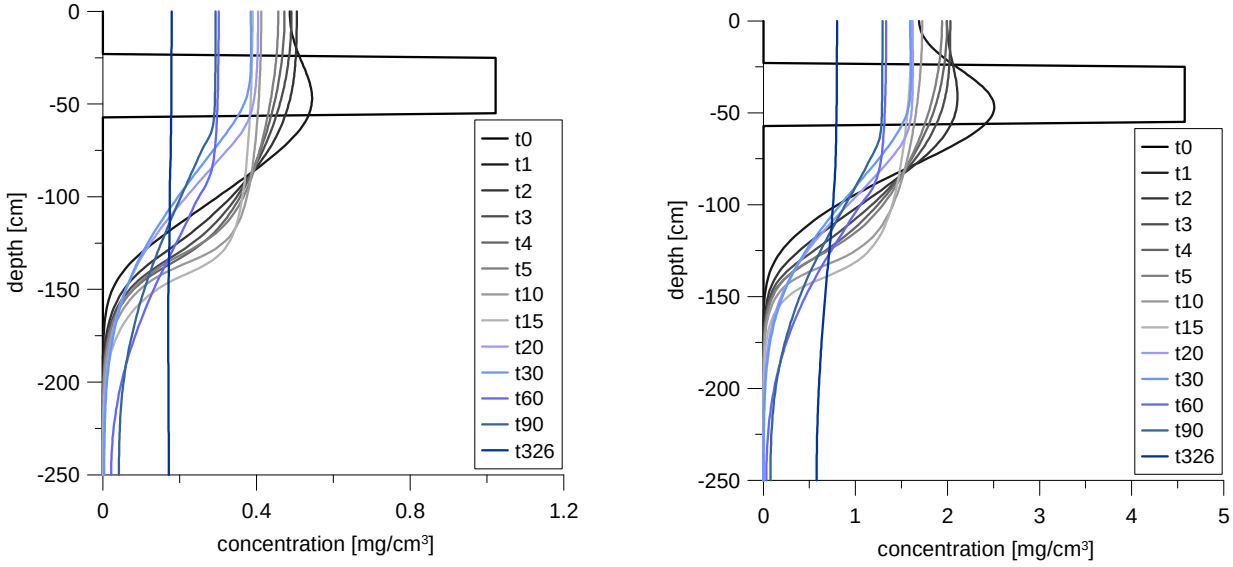

Figure 15: Distributions of benzene (left) and xylenes (right) versus depth for the variable water table

However, although the water table after 30 days is at -80 cm, the downward movement of the BTEX compounds is not sufficiently hindered by their lower molecular diffusion coefficients in water as compared to ethanol. Hence the BTEX spreads equally over the entire depth range. Figure 16 shows the distribution of the E85 mixture versus time at the observation nodes at depths of 90, 145 and 160 cm bgs. Concentrations of all components in the E85 mixture increase rapidly at 90cm, with small peaks visible just above the

capillary fringe. After water table has risen to 80 cm bgs, the concentrations of all species decrease sharply, both at the former capillary fringe and at 90cm bgs. It is important to notice that now also the upper observation node is under saturated conditions. The ethanol concentrations at 160cm bgs, for the case of a variable water table remain fairly constant and are comparable to concentrations observed for the constant water table scenario. Only approximately 150 days after release of the E85 mixture do the ethanol concentrations in the case of a variable water table at 160cm become higher than in the case of a constant water table.

For the BTEX compounds, the variable water table smears out the concentration differences which is present in the case of a constant water table (i.e. concentrations present above the initial capillary fringe are lower, and concentrations below the initial water table are higher) compared to the model with a constant water table.

5.3. Relation to other studies

Results obtained in this study about the retainment of E85 in the case in of a constant water table seem to be in correspondence with those by Mc Dowell et al. [2003]. However, Freitas et al [2011] mentioned that the extent of retainment in the unsaturated zone depends on the volume of the spill and that with increasing volumes more ethanol should reach the capillary fringe. Since Mc Dowell et al. [2003] only considered a small spill, a large part of this volume should be retained. However, TDR measurements by Schneider and Corseuil [2012] on the same E85 field site as the one used in this study showed that even for a large volume spill the E85 mixture initially is retained in the unsaturated zone (figure 17). At least until a water table rise of 0,8 m occurred. However the increase in ethanol fractions observed in their paper was larger than the relative increase in ethanol concentrations observed in this study. Nonetheless, in correspondence with Schneider and Corseuil [2012], model predictions of this study indicate that water table oscillations will aid in the migration of ethanol to greater depths of the saturated zone.

Still, the equal spreading of the E85 mixture over the entire depth of the profile as observed in figures 14 and 15 may not necessarily occur in all field situations. This is due to the fact that there may be significant lateral transport through the capillary fringe (e.g. Freitas et al. [2011], Stafford et al. [2009]) which may move ethanol and BTEX compounds from the source area and hence diminish migration into the saturated zone below the source. Also, the assumption made is made here that the E85 mixture is immediately dissolved into the liquid phase upon release into the subsurface. This neglects possible downward movement of ethanol as a pure phase and could lower the volumes of dissolved ethanol reaching the capillary fringe. On the other hand, this initial equilibrium assumption may lead to faster diffusion in the water phase and as such underestimate vaporization of E85 from the pure phase.

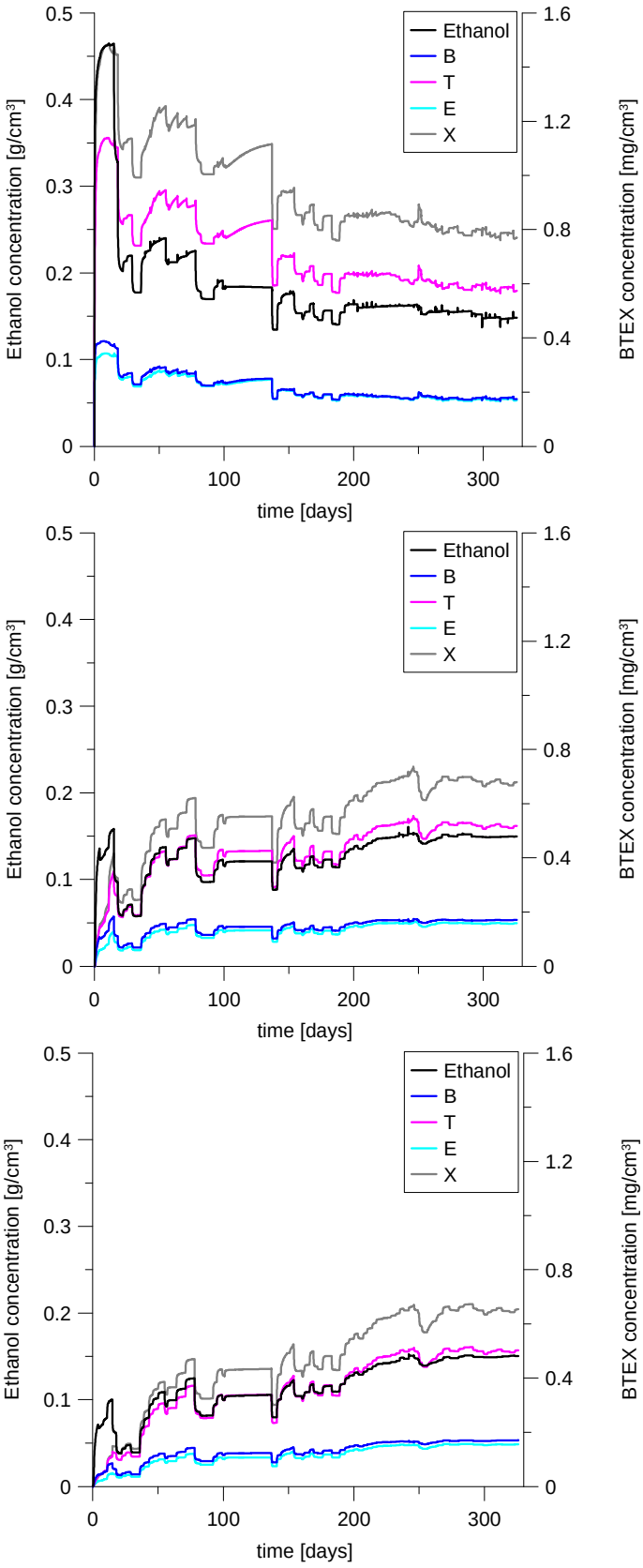

Figure 16: Ethanol and BTEX concentrations at depths of 90 cm (top), above the capillary fringe at 145 cm (middle), and at the water table at 160 cm (bottom)

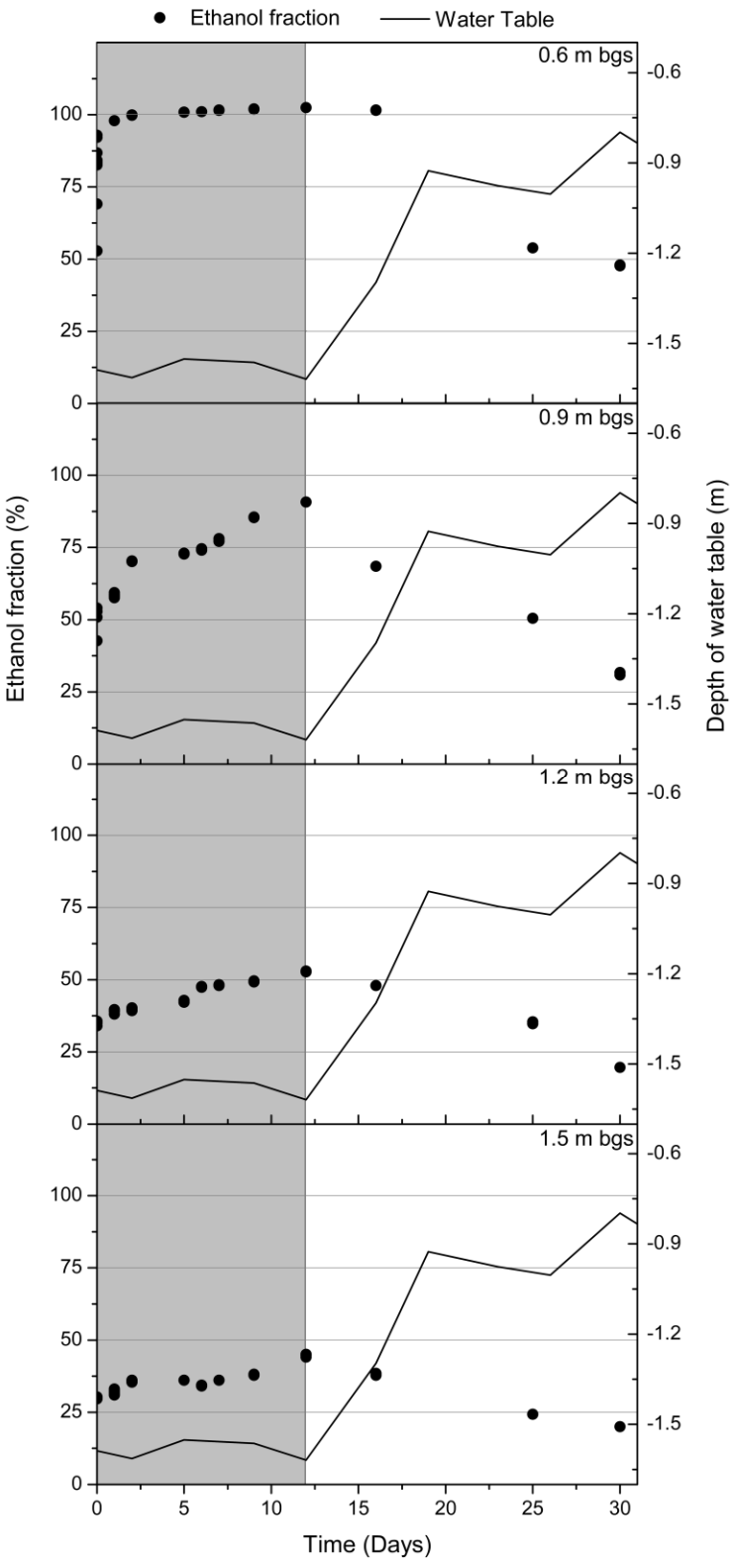

Figure 17: Ethanol fraction in source zone and water table fluctuation in 30 days of experiment. Dark region represents the first 12 days of experiment (picture taken from Schneider and Corseuil [2012])

6. Sensitivity Analysis

In this section the effects of several processes and transport parameters are investigated. No detailed sensitivity analysis is provided in the classical sense, including an uncertainty analysis. Rather, the effects are shown of several different experimental scenarios and a selected few parameters changes. These include having no plastic cover on the soil surface after release of the E85 mixture assuming both a constant and variable water table (sections 6.1 and 6.2, respectively), having a different stagnant diffusion length (d) above the soil surface that would alter volatilization rates into the atmosphere (section 6.3), and changes in the gaseous diffusion coefficient (section 6.4) and Henry's constant (section 6.5).

6.1. No plastic cover; constant water table

To assess the effect of not having a plastic cover on top of the E85 field source area, the upper boundary condition for transport was modified to account for volatilization as described by Equation (17) in section 4.2, but with a gas phase concentration of zero in the atmosphere (g_{atm}). For the water flux (q), equation (14) was used, in which $q_o(t)$ was calculated from available precipitation and potential evaporation data a explained in section 4.2 using system-dependent (atmospheric) soil surface boundary conditions as implemented in HYDRUS-1D (Simunek et al., 2008). Following Jury et al. [1983], all calculations were carried out using a value of 0.5 cm for the stagnant diffusion length, d. This scenario would simulate a spill from a leaking fuel pipeline in an open terrain, rather than a leak below a gasoline station.

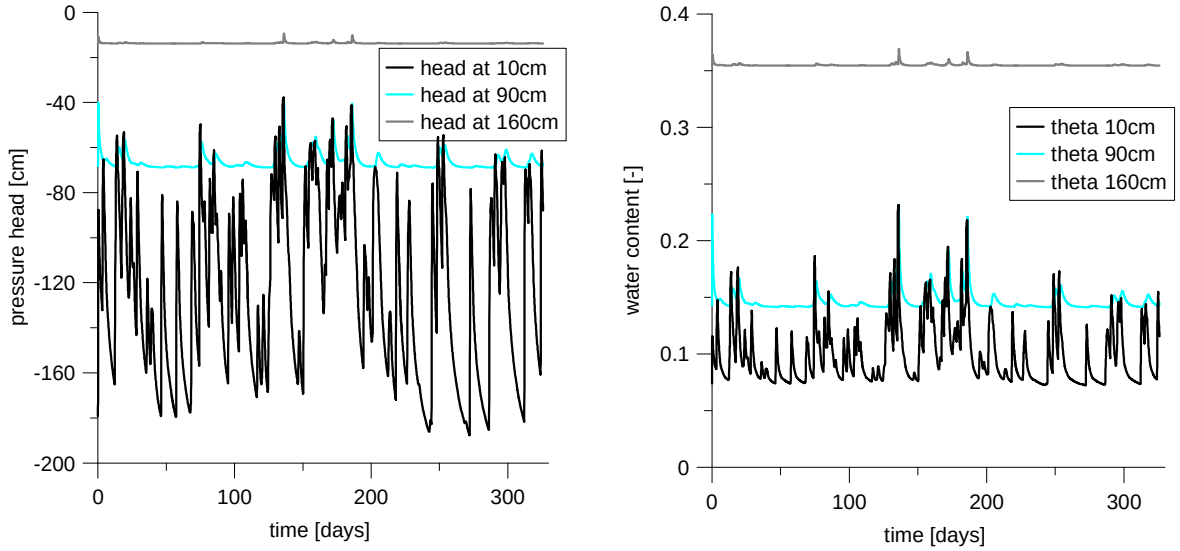

Figure 18: head and water content profiles at different depths for a constant water table, assuming no plastic cover on the soil surface

Results for the model with constant water table which now include precipitation and volatilization (figure 18) show that the precipitation alters the pressure head and the water content at a depth of 10cm drastically.

However, at 90cm this effect is not so pronounced. This can also be seen in figure 19 where distributions of pressure and water content versus depth seem to be unaltered below a 100cm depth for the entire simulated period

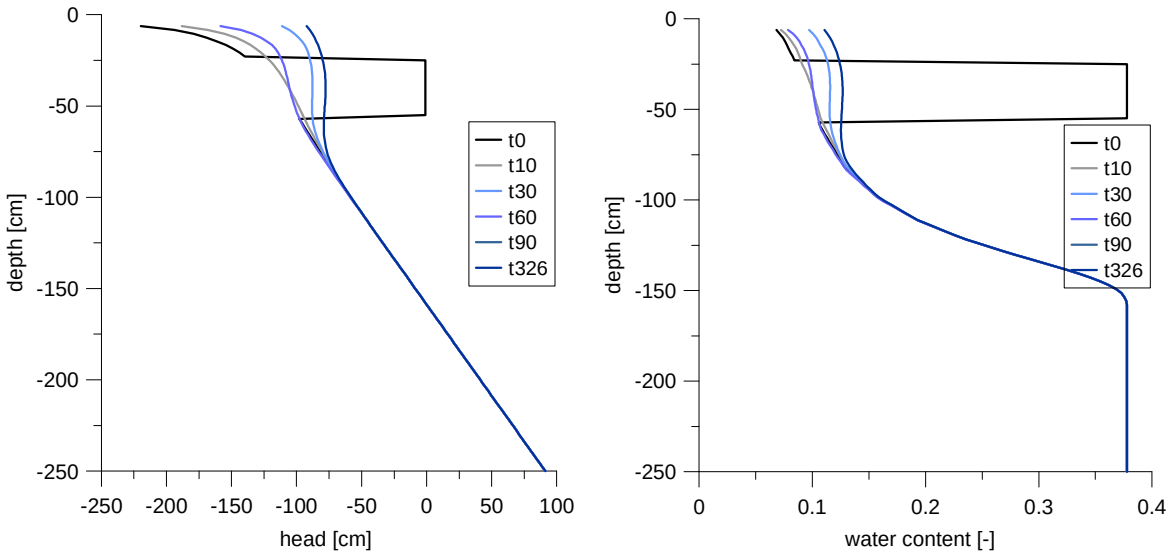

Figure 19: Distributions of pressure head and water content versus depth for a constant water table, assuming no plastic cover on the soil surface.

Nonetheless, ethanol moves much more rapidly downward as compared to the constant water table scenario with plastic on top (figure 10). The bulk of the ethanol reaches the water table after approximately 30 days. After 90 days the peak in concentration is at the water table and a considerable amount of ethanol is in the saturated zone.

Distributions for benzene and xylenes are very similar to those for ethanol. However, after 15 days concentrations of the BTEX components (fig. 21) are two times lower than those for the original constant water table scenario. Nonetheless, results show that the BTEX compounds do move deeper into the profile when precipitation is present, while volatilization from the soil surface at the same time can cause significant depletion of the BTEX compounds within the time of simulation.

Another reason for the fast downward movement of ethanol and BTEX may be the constant water table itself. When the water table is kept constant and saturation at the top increases due to rainfall, and if gaseous diffusion is equally important as for the original scenario, BTEX is pushed downwards due to the incoming precipitation. This certainly will hinder volatilization initially but should not prevent the escape of the BTEX compounds over time during relatively dry periods.

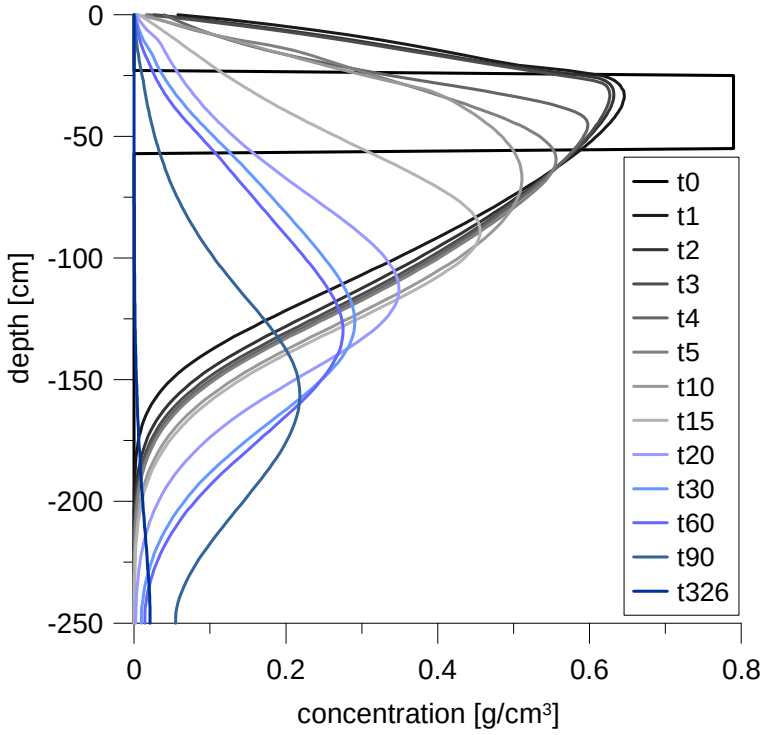

Figure 20. Distributions of ethanol versus depth for a constant water table, assuming no plastic cover on the soil surface.

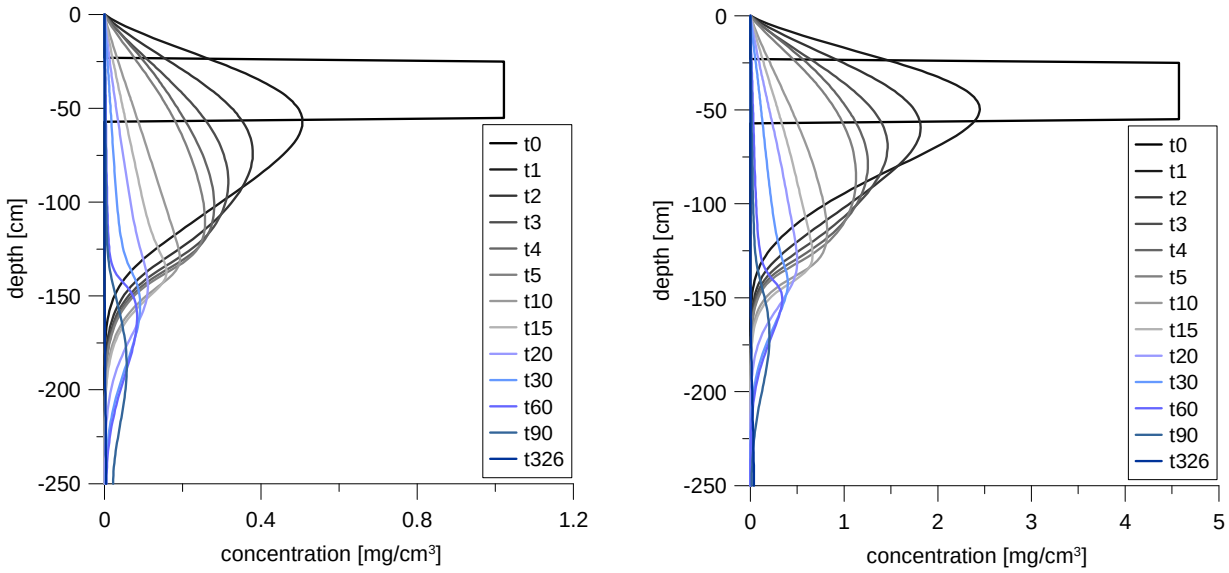

Figure 21. Distributions of benzene (left) and xylenes (right) versus depth for a constant water table; assuming no plastic cover on the soil surface.

Distributions versus time (figure 22) show depletion of BTEX within 150 days at a depth of 90cm bgs. For ethanol this process is somewhat slower but still within 200 days after release of the E85 mixture. The observation nodes at depths of 145 and 160 cm also show depletion of both ethanol and BTEX.

Figure 20 showed that a large part of the ethanol in the profile was located close to the water table 90 days after release. It is unlikely that all ethanol will have volatilized. Some of the ethanol may have moved also downwards out of the profile to depths below 250 cm. Although not further shown here, an observation node placed at 250cm bgs confirmed this leaching below the lower boundary, with a peak in concentration occurring approximately 150 days after release. At this time the ethanol and BTEX concentrations at all observation nodes had dropped significantly.

To get a better view of the importance of volatilization, the fluxes of ethanol and the BTEX components leaving the model domain are shown in figure 23. It can be seen that volatilization only occurs at early stages after the release of E85, and that volatilization has become negligible within 100 days. The cumulative surface flux shows that volatilization is much more important for BTEX than for Ethanol. This can be verified by simply multiplying the cumulative surface flux by the area of release (table 3) and then comparing it to the mass released (table 2). Results of this simple computation show that volatilization may lead to a loss of about 16% of the ethanol. For all of the BTEX components, volatilization accounts for a loss of more than 95% of the total amount initially present.

These results must be viewed with caution because of the assumption in this study that all BTEX released is fully dissolved in ethanol, which in turn is fully dissolved in water at the start of the experiment. This process normally would require some time. Furthermore, in the field experiment the 170L of ethanol released may entrap some of the BTEX and thus prevent it from moving upward and volatizing.

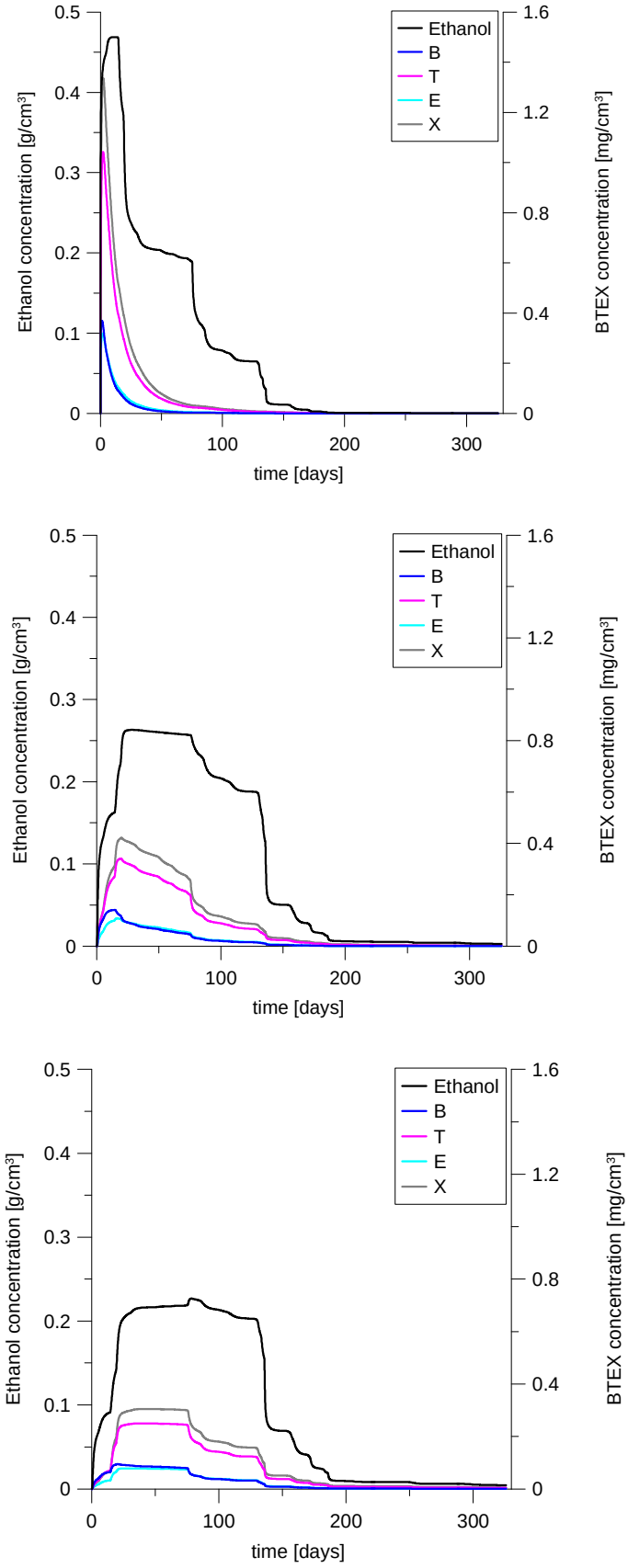

Figure 22: Ethanol and BTEX concentrations at depths of 90 cm (top), above the capillary fringe at 145 cm (middle), and at the water table at 160 cm (bottom) for a constant water table, assuming no plastic cover on the soil surface.

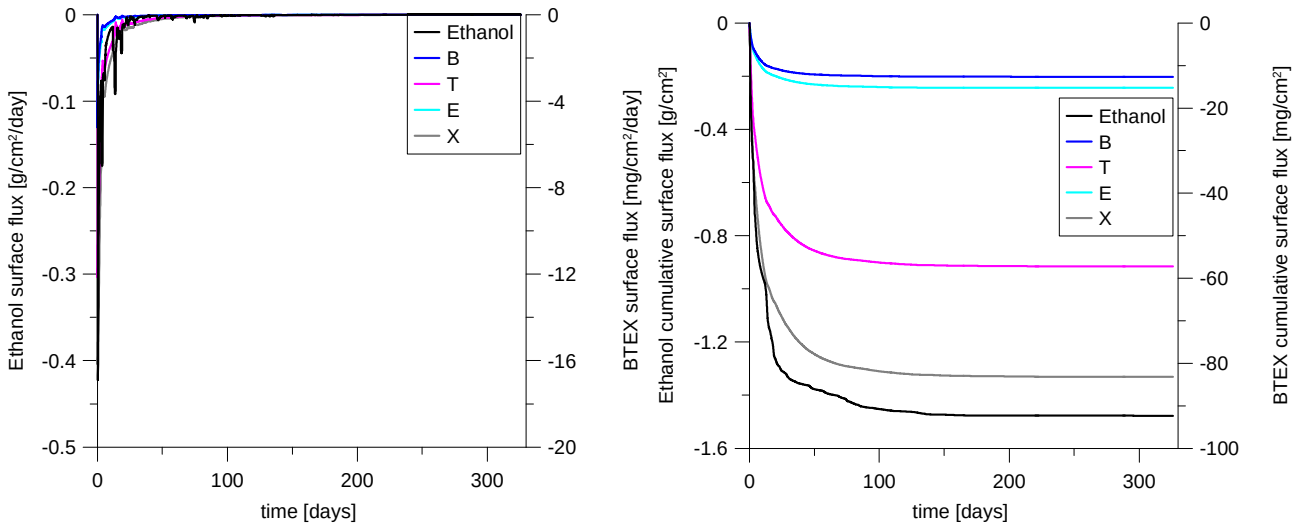

Figure 23. Ethanol and BTEX fluxes leaving the region (negative flux) at the upper boundary of the system. The right-hand figure represents cumulative fluxes (constant water table scenario).

6.2. No plastic; variable water table

For the model with a variable water table the effects of the plastic were also investigated. The pressure head and water content profiles (figure 24) are very similar to the profiles shown in figure 13. The only difference is that precipitation creates an erratic pattern in both the water content and pressure head profile at 10cm depth. The distributions of the pressure head and water content show that with both precipitation and assuming no plastic on the soil that the initial pressure head and water content are redistributed across the profile within 10 days.

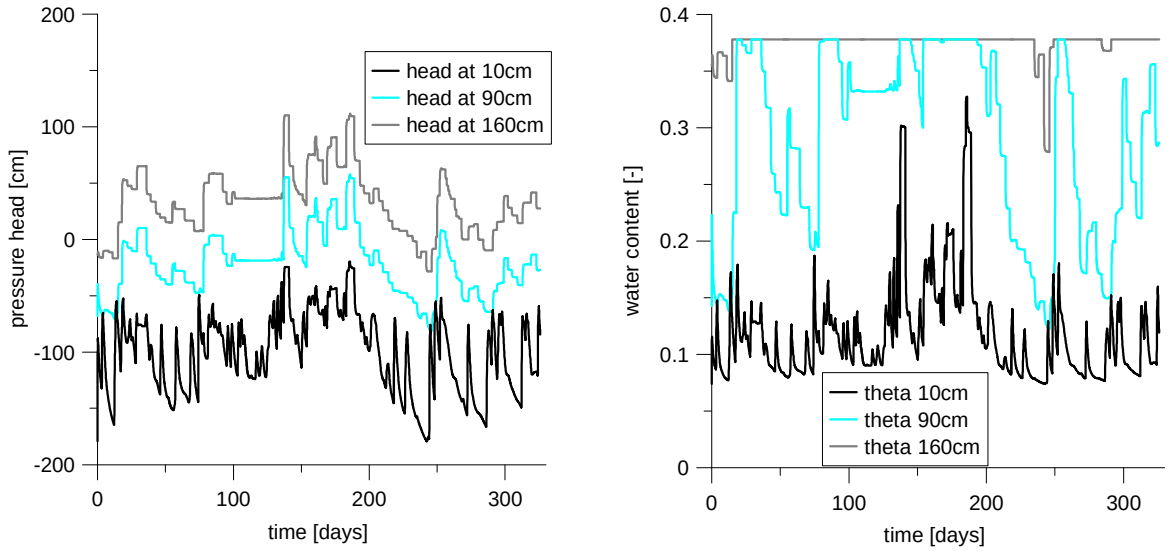

Figure 24: head and water content profiles at different depths for a variable water table, assuming no plastic cover on the soil surface

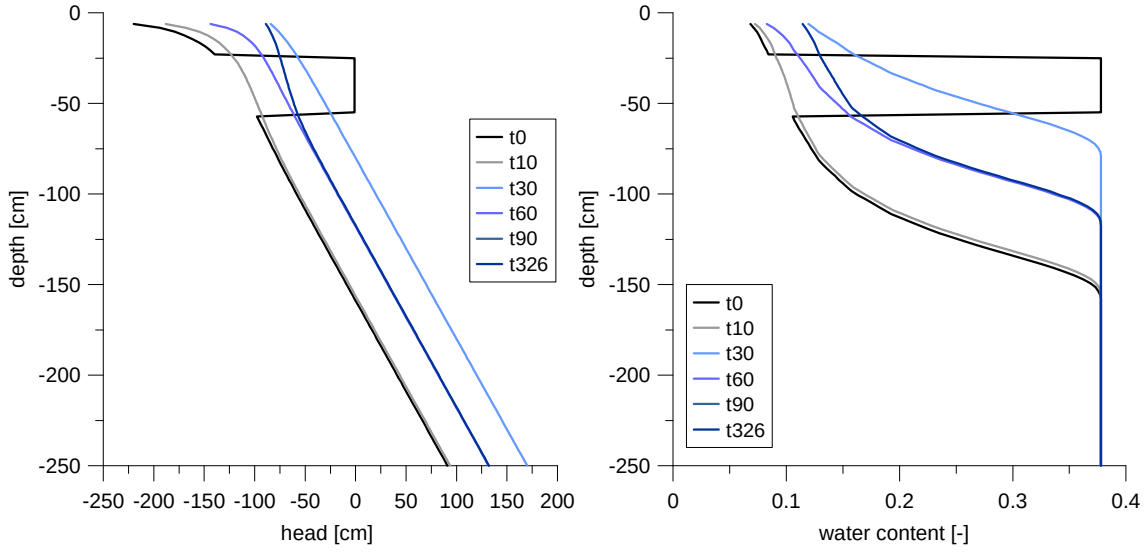

Figure 25: Distributions of pressure head and water content versus depth for a constant water table, assuming no plastic cover on the soil surface.

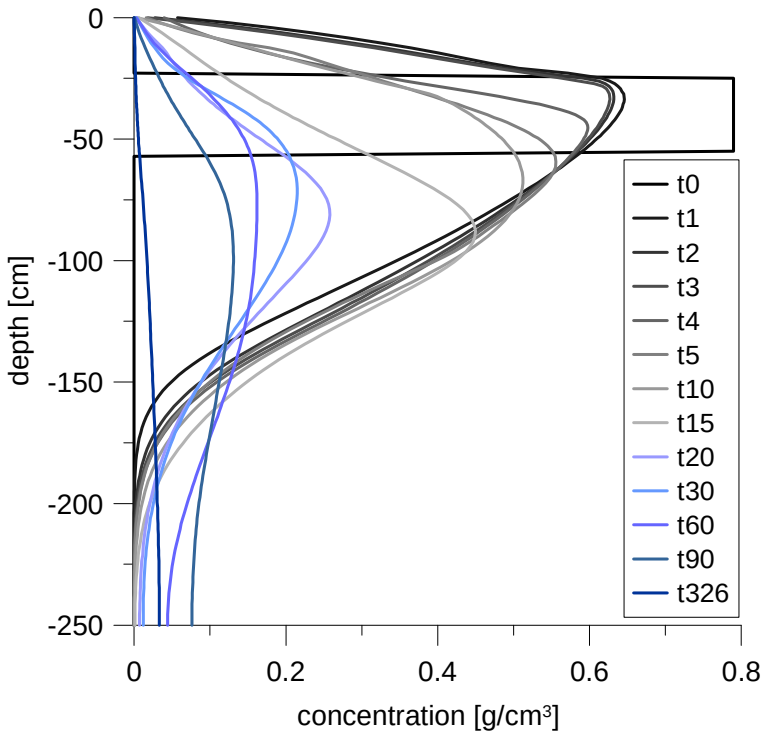

Figure 26. Distributions of ethanol versus depth for a variable water table, assuming no plastic cover on the soil surface.

The distribution of ethanol versus depth (figure 26) shows a similar trend for the first 15 days compared to the model with a constant water table and precipitation. 20 days after the release the bulk of ethanol is at 80 cm bgs, which is again at the water table due to the rising water table. Since the water table fluctuates between 80 and 120 cm for approximately the next 100 days, the bulk of ethanol remained roughly at 80 cm bgs, although also downward movement of ethanol occurred. This leads to a more spread out concentration and eventually after 90 days concentrations are even slightly higher compared to the constant water table scenario (fig 20) which also assumed that no plastic was present.

Comparing the results of ethanol to the initial scenario with only a variable water table (fig 14) it can be seen that 20 days after the release the bulk of ethanol has moved 50 cm deeper into the profile. However, concentrations at 80 bgs are only slightly elevated when the plastic is removed. Another striking difference is the concentration distribution at the end of the simulation. The concentration of ethanol for the initial scenario is equally distributed with depth whilst including precipitation into the model caused the ethanol concentration to drop to values close to zero across the profile. Although precipitation is obviously a major reason for the observed effects, the invoked lower boundary conditions likely also played a role. This because the lower boundary condition for both models (with and without plastic) was set to be a zero concentration gradient. This means that when water is not leaving the system, ethanol and BTEX should also

stay within the system. With plastic on the soil surface, the downward liquid flow rate is very small which means that little or no ethanol and BTEX will be leaving the system. However, when the plastic is removed, precipitation will increase the liquid flow rate and ethanol and BTEX can leave the model domain.

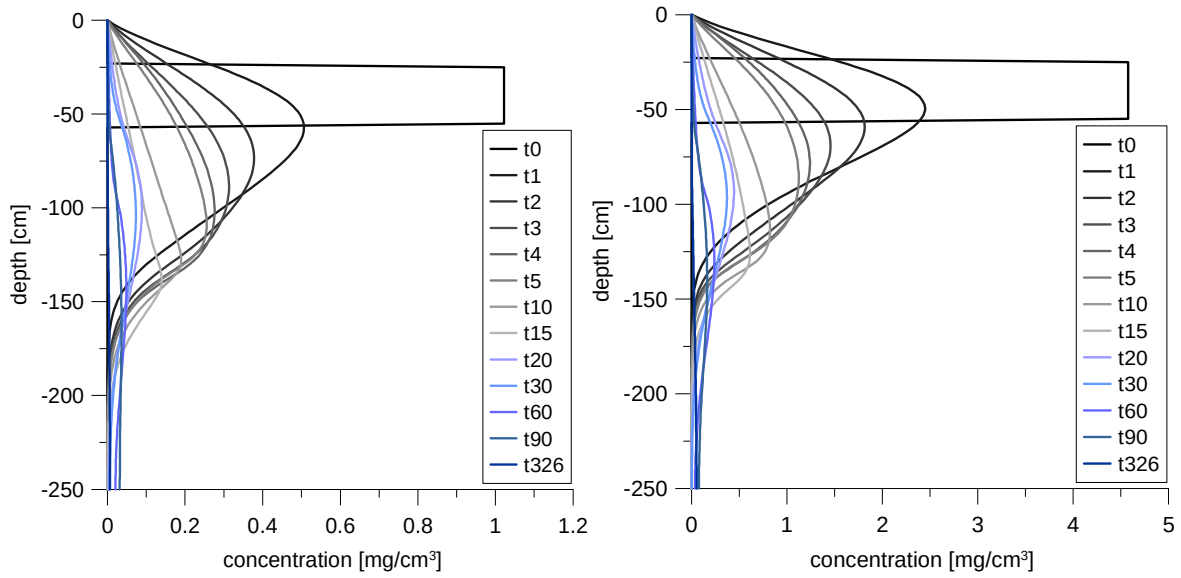

Figure 27. Distributions of benzene (left) and xylenes (right) versus depth for a variable water table; assuming no plastic cover on the soil surface.

Besides increased leaching, removal of the plastic will also lead to volatilization of the BTEX compounds (fig 27), leading to even faster decreasing BTEX concentrations than for the case with a constant water table and precipitation. However, although the results are only marginally different, concentrations of BTEX seem to be slightly elevated deeper into the profile compared to the constant water table scenario without plastic. The observation node at 90 cm (fig 28) shows that including precipitation and a variable water table may lead to lower concentrations for all species when compared to the scenario with only a variable water table, with exception for the first 40 days. At depths of 145 and 160 cm concentration also seem to be slightly elevated when compared to the variable water table scenario.

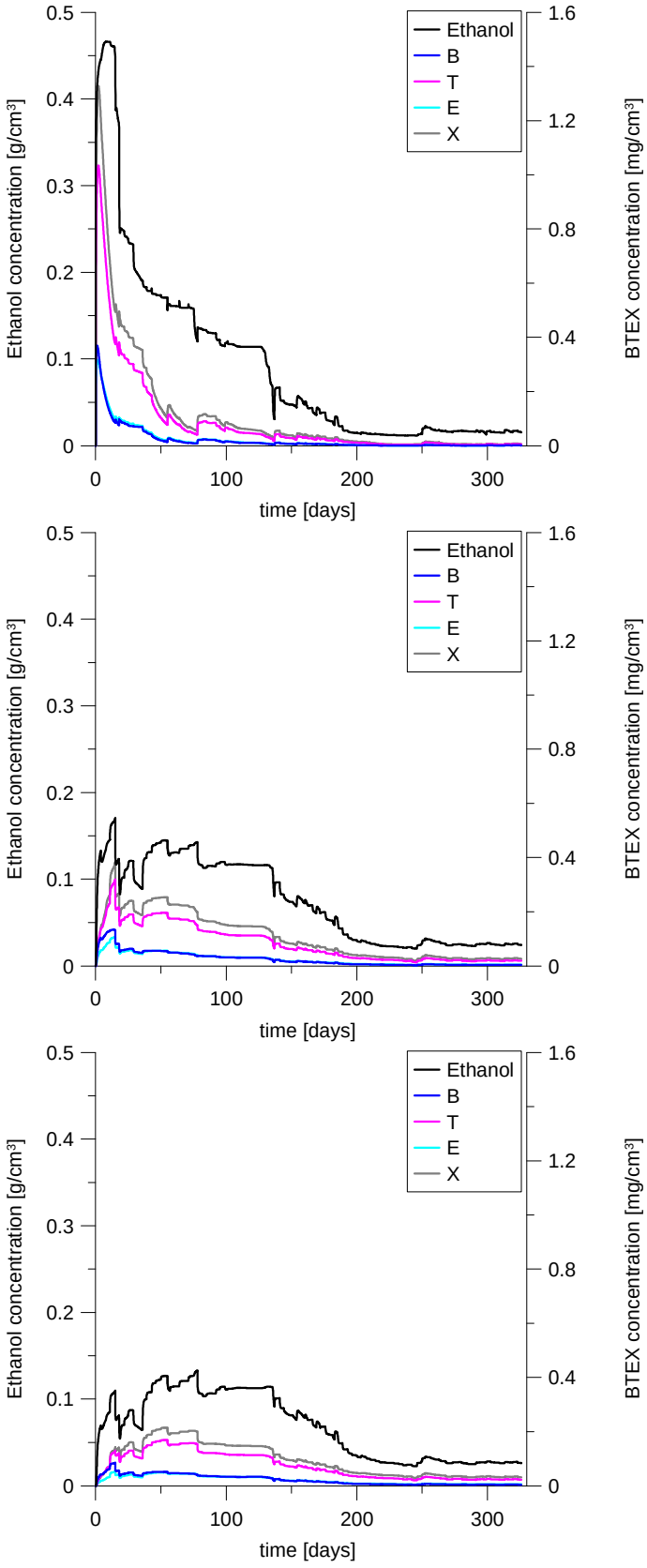

Figure 28 Ethanol and BTEX concentrations at depths of 90 cm (top), above the capillary fringe at 145 cm (middle), and at the initial water table at 160 cm (bottom) for a variable water table, assuming no plastic cover

To also obtain a better view of the importance of volatilization for this scenario, the fluxes of ethanol and the BTEX components leaving the model domain are shown in figure 29. Results indicate that volatilization now occurs for a longer period of time after release of E85 compared to figure 23, with the volatilization rate becoming negligible within 200 days after the initial release. Again, the cumulative surface flux shows that volatilization is much more important for BTEX than for ethanol, and that for all of the BTEX components volatilization accounts for a loss of more than 95% of the total amount initially present. For ethanol volatilization increased to 30% of the total amount released. This may be due in part to the rising water table, which pushed the bulk of ethanol upwards, thus making ethanol more susceptible to volatilization from the soil surface.

Comparing the two models that include precipitation and evaporation, the behavior at a depth of the various contaminants at 90 cm seems to be almost identical. The major difference is that figure 28 indicates that there is still some ethanol present at the end of the simulation, whilst the observation nodes of figure 22 show that ethanol is virtually depleted after 200 days. A preliminary conclusion therefore may be that implementing a variable water table tends to smear out the concentration over the modeled domain, with diffusion in the gas phase being the main process, with precipitation being the major process moving the species downwards out of the modeled domain.

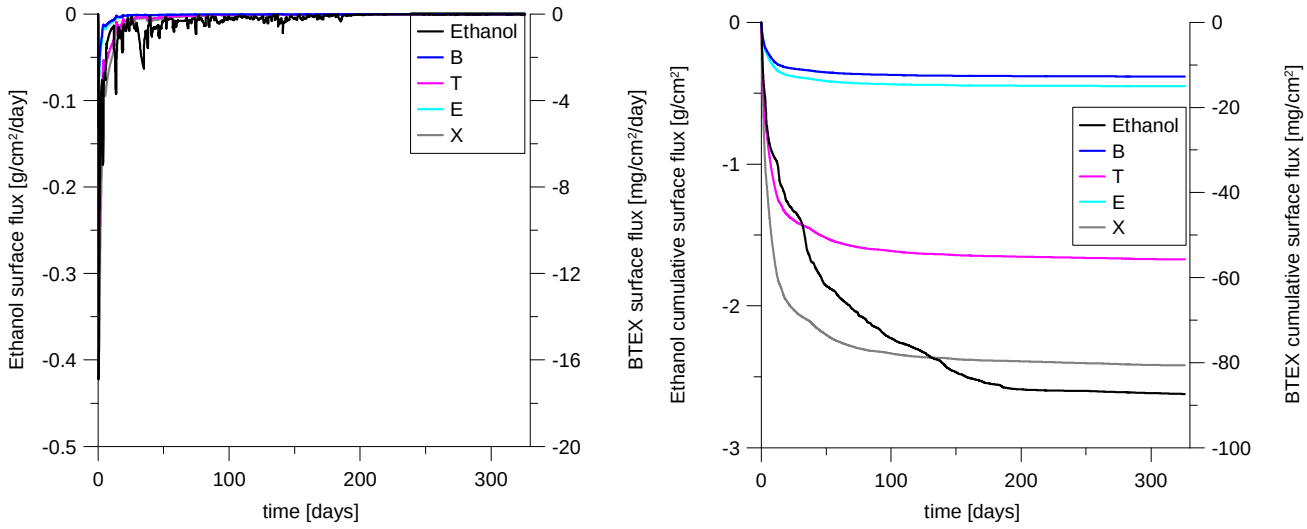

Figure 29. Ethanol and BTEX fluxes leaving the region (negative flux) at the upper boundary of the system. The right-hand figure represents cumulative fluxes (variable water table scenario).

6.3. Stagnant boundary layer

The length of the stagnant boundary layer (*d*) affecting the volatilization rate from the soil surface was taken originally to be 0.5 cm after Jury et al. [1983]. This value may have an important effect on the amount of volatilization. The importance of the diffusion length was investigated by doubling and halving the original value of 0.5 cm. Note that the diffusion length is only important for models which do not have the plastic on top of the soil surface, since the plastic prevents gases from escaping.

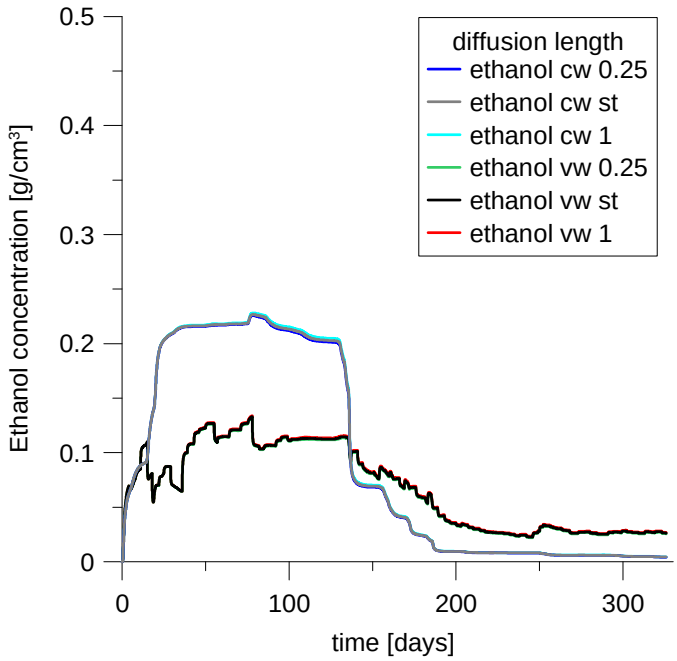

Figure 30. Effect of the thickness (*d*, in cm) of the stagnant boundary layer on the concentration of ethanol at a depth of 160 cm. The standard scenario (st) is for d=0.5 cm. In the figure, cw and vw represents the constant and variable water table scenarios, respectively.

Figure 30 shows the effects of the stagnant boundary layer (*d*) on ethanol concentrations at a depth of 160 cm. The plots indicate that when the plastic is removed the value of *d* has no influence on the concentrations of ethanol in both models. Results at other depths and the BTEX compounds are omitted in this section since there was no observed effect of the diffusion length for these scenarios as well.

6.4. Gas diffusion coefficient

The sensitivity to the gas diffusion coefficient (dif g, or D_g) was investigated by varying the standard values of table 2 by ± 1000 cm^2 d^{-1}. For all models there was very little difference in the computed ethanol concentration for the implemented changes in D_g; hence results are not presented here.

However, the BTEX compounds showed some sensitivity to alterations in D_g. Figure 31 shows the effect of changing D_g for the variable water table scenario, with the other scenarios all showing very similar effects. The effects for the xylenes were somewhat more pronounced than for those for the benzenes for which alterations in D_g were nearly negligible. Although the effects of the gas diffusion coefficient do not seem too important, it is interesting to note that altering D_g has the reversed effect on models without precipitation (I and II) compared to the models that include precipitation and evaporation (III and IV). This suggests that increasing D_g leads to faster gas diffusion when the plastic is present on top, which in turn leads to higher concentrations at depth. When the plastic is removed, increasing D_g may have the opposite effect since this may lead to extra volatilization and hence lower concentrations at depth.

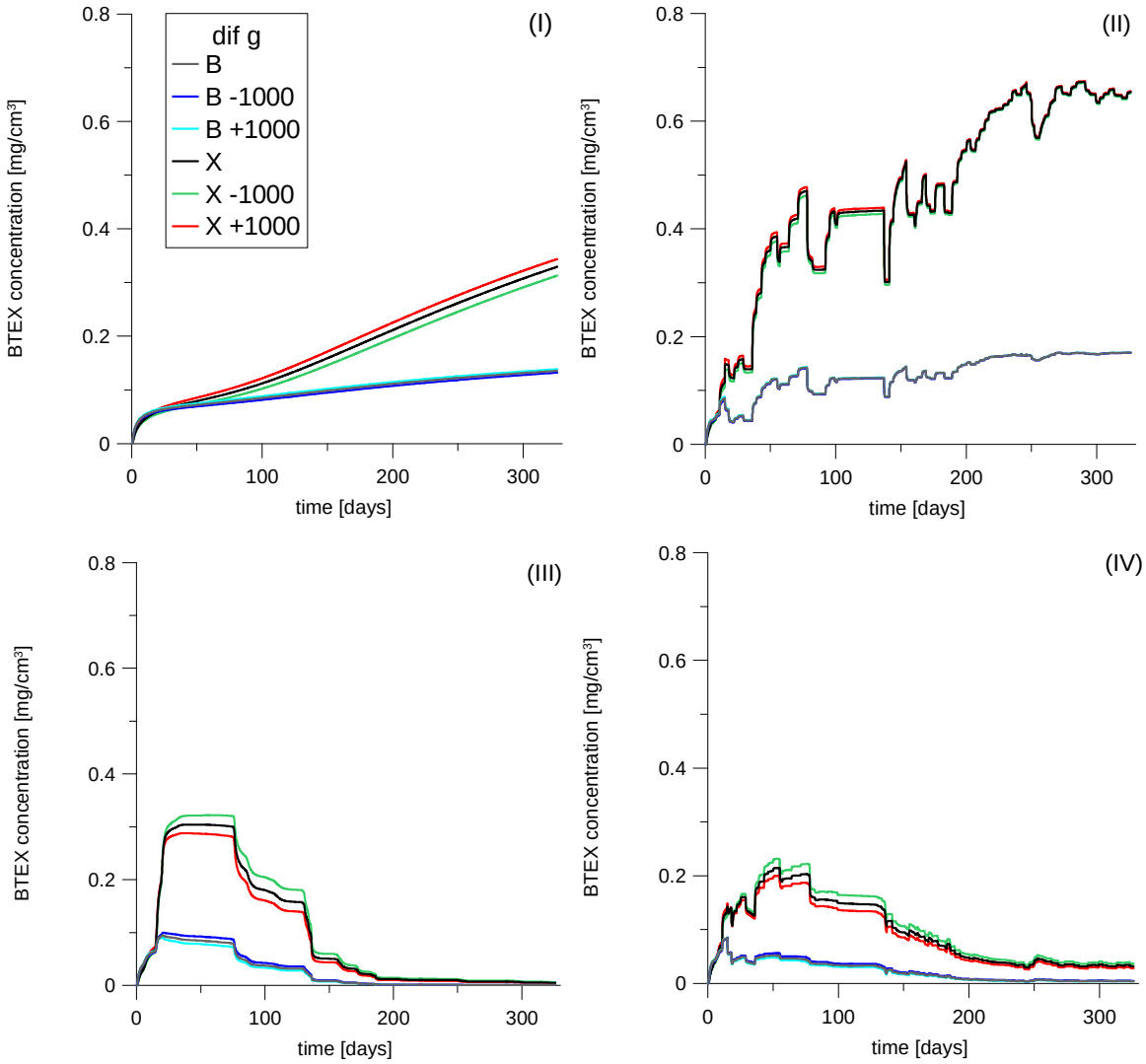

Figure 31. Effect of D_g on the concentration of BTEX for a (I, III) constant and (II, IV) variable water table with (III, IV) and without (I, II) precipitation at a depth of 160cm. B stands for Benzene and X for Xylenes.

6.5. Henry's constant

Another important parameter controlling gas diffusion is Henry's constant. As can be seen in table 2 Henry's constant for ethanol is 3 to 4 orders of magnitude smaller that for the BTEX compounds. For this reason it should be expected that doubling Henry's constant for sensitivity analysis will have very little effect. Although results are not presented here, sensitivity analysis indeed showed that altering Henry's constant for ethanol had no effect, as was already inferred from figures 4 to 6. This immediately explains why changing D_g for ethanol had no effect on the predicted concentrations of the model since little ethanol vaporizes anyway, with the rate which the gas constituent moves not significantly altering the amount of ethanol present at any point in the system.

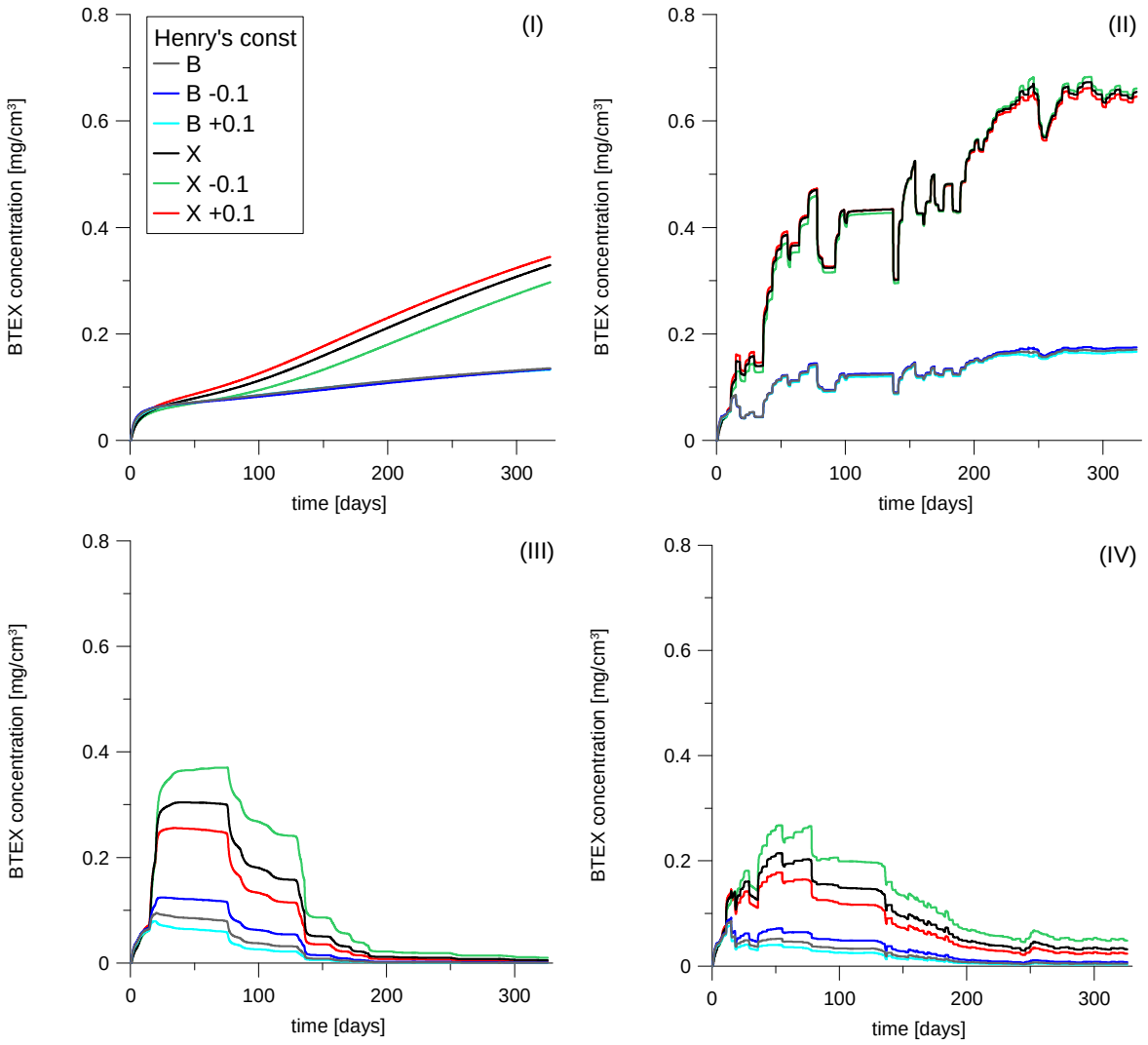

Figure 32: effect of Henry's constant on the concentration of BTEX for a (I, III) constant and (II, IV) variable water table with (III, IV) and without (I, II) precipitation at a depth of 160cm. B stands for Benzene and X for Xylenes.

However, figure 21 shows that BTEX concentrations are relatively sensitive to alterations in Henry's constant of ±0.1, with the exception of figure 32 (II), which is the model for a variable water table. Furthermore, as is the case for D_g, it can be seen that altering Henry's constant has a reversed effect on the model without precipitation (I) compared to the models that include precipitation and volatilization (III and IV). The reasons for this may be that with less BTEX in the gas phase, BTEX concentrations for fig 32(III) and (IV) are larger at depth due to smaller losses caused by vaporization, whilst for the model with plastic on top less BTEX in the gas phase leads to less spreading across the profile since no gas volatilizes. Keeping in mind that the field site was covered by plastic, and had a variable water table, one may conclude on basis of figures 31 and 32 that this model is least susceptible to changes in parameters controlling gas diffusion.

7. Conclusions

In this paper several models were constructed to simulate the effects of a spill of 200L E85 in the unsaturated zone from a controlled release field experiment of the Federal University of Santa Catarina, Brazil. Results from the models suggest that without water table fluctuations ethanol and BTEX are retained in the unsaturated zone. In correspondence with findings by Schneider and Corseuil [2012], model predictions further indicate that water table oscillations cause the migration of ethanol to somewhat greater depths in the saturated zone. However, the results show equal spreading of E85 over the entire depth of the profile, something which is not likely to occur in the field experiment if horizontal transport through the capillary fringe will remove ethanol and BTEX compounds. Furthermore, some of the equal spreading of ethanol may be caused by the boundary conditions implemented in the model. These boundary conditions cause E85 to remain within the system due to a very small liquid flow rate. Sensitivity analyses showed that removing the plastic on the soil surface may increase volatilization from the soil surface as well as increased downward movement of ethanol and BTEX. Furthermore, model predictions suggest that the increased liquid flow rate allows ethanol and BTEX to move out of the modeled domain. Sensitivity analyses further suggests that, although volatilization may be important for BTEX, altering the parameters which control gas diffusion do not have a major effect on the results. Moreover, the model for a variable water table and plastic on top of the soil surface (i.e. the model that represents the actual field experiment) is least affected by changes in the gas diffusion parameters.

Another assumption was made in the modeling efforts that the E85 mixture is immediately dissolved into the liquid phase upon release into the subsurface. This assumption does not allow one to study the effects of cosolvency. Furthermore, future research is required to investigate the effects of biodegradation over long periods of time. Further research should also focus on lateral transport, including water table oscillations as carried out in this study, which will require the use of two- or even three-dimensional models.

8. Acknowledgements

The author is grateful to Prof. Dr. M.T. van Genuchten for his criticism and reviewing this paper in its early stages as well as providing helpful comments and tips during modeling with Hydrus-1D. Furthermore the author acknowledges Prof. Henry X. Corseuil for useful discussions and the people from REMAS of the Federal University of Santa Catarina for providing essential data required for this study. Financial support for this project was provided by the K.F. Hein Foundation and Stichting Molengraaff Fonds.

9. References

Alimi-Ichola, I., Gaidi, L. "Influence of the unsaturated zone of soil layer on the solute migration." Engineering Geology, 2006, vol. 85 pp. 2–8.

Brooks, R. H., and A. T. Corey. 1964. Hydraulic properties of porous media, Hydrol. Paper No. 3, Colorado State Univ., Fort Collins, CO.

Chen. C.S., Lai, Y., Tien C., "Partitioning of aromatic and oxygenated constituents into water from regular and ethanol-blended gasolines." Environmental Pollution, 2008, vol. 156 pp. 988–996.

Chung S. O., Horton, R. "Soil heat and water flow with a partial surface mulch." Water Resour. Res., 1987, vol. 23(12), pp. 2175-2186.

Corseuil, H.X., Alvarez, P.J.J. "Natural bioremediation perspective for BTX-contaminated groundwater in Brazil" Water Sci. Technol. 1996, vol. 35, pp. 9-16

Corseuil, H.X., Hunt, C.S., Santos R.C.F., Alvarez P.J.J. "The influence of the gasoline oxygenate ethanol on aerobic and anaerobic BTX biodegradation". Water Res. 1998, vol. 32(7), pp. 2065–72.

Corseuil, H.X., Kaipper, B.I.A., Fernandes, M. "Cosolvency effect in subsurface systems contaminated with petroleum hydrocarbons and ethanol". Water research 2004, vol. 38, pp. 1449-1456.

Corseuil, H.X., Schneider, M.R., do Rosário, M. "Natural attenuation rates of ethanol and BTEX compounds in groundwater contaminated with gasohol". Appropriate Environmental and Solid Waste Management and Technologies for Developing Countries, 2002, vol.4, pp. 2121-2128.

Dakhel, N., Pasteris, G., Werner, D., Höhener, P. "Small-volume releases of gasoline in the vadose zone: impact of the additives MTBE and ethanol on groundwater quality." Environmental Science & Technology, 2003, vol. 37, pp. 2127–2133.

Durner, W. 1994. Hydraulic conductivity estimation for soils with heterogeneous pore structure, Water Resour. Res., 32(9): 211-183.

Freitas, J.G., Barker, J.F. "Monitoring Lateral Transport of Ethanol and Dissolved Gasoline Compounds in the Capillary Fringe" Ground Water Monitoring & Remediation, 2011, vol.31(3) pp. 95–102

GL (Global Lightning) Technologies, “Lightning Protection Standards AS/NZS1768-1980”, various appendix, O'Connor, Australia, 1980

Heermann, S.E, Powers, S.E. “Modeling the partitioning of BTEX in water-reformulated gasoline systems containing ethanol”. J ContamHydrol 1998, vol. 34(4) pp. 315-341.

Hunt, C.S., Alvarez, P.J.J., Ferreira dos Santos, R.C., Corseuil, H.X. “Effect of ethanol on aerobic BTEX degradation.” In *In Situ and On-Site Bioremediation* ed. B.C. Alleman and A.L. Leeson., 1997, vol. 4(1) pp. 49–54

IMKO Micromodultechnik GmbH, “Theoretical Aspects on Measuring Moisture Using TRIME”, Ettlingen, Germany, 2006

Ingram, L. and Buttke, T. “Effects of alcohols on micro-organisms.” Advances in Microbial Physiology, 1984, vol.25, p.253.

Kosugi, K. 1996. Lognormal distribution model for unsaturated soil hydraulic properties, Water Resour. Res., 32(9): 2697-2703.

Lage, I. Msc Thesis: avaliação de metodologias para determinação da permeabilidade em meios porosos, 2005

Mualem, Y. 1976. A new model for predicting the hydraulic conductivity of unsaturated porous media. Water Resour. Res. 12:513–522.

Mackay, D.M., de Sieyes, N.R., Einarson, M.D., Feris, K.P., Pappas, A.A., Wood, I.A., Jacobson L., Justice, L.G., Noske, M.N., Scow, K.M., Wilson, J.T., “ Impact of ethanol on the natural attenuation of benzene, toluene, and o-xylene in a normally sulfate-reducing aquifer.” Environmental Science and Technology, 2006, vol. 40(19), pp 6123–6130.

Marquardt, D. W., “An algorithm for least-squares estimation of nonlinear parameters”, SIAM J. Appl. Math., 1963, vol.11, pp.431-441.

McDowell, C.J., Powers S.E. “Mechanisms Affecting the Infiltration and Distribution of Ethanol-Blended Gasoline in the Vadose Zone”. Environ Sci Technol 2003, vol. 37, pp. 1803-1810

Niven, R. K. “Ethanol in gasoline: environmental impacts and sustainability review article”. Renewable and Sustainable Energy Reviews, 2005, vol. 9, pp. 535–555.

Österreicher-Cunha, P., do Amaral Vargas Jr., E., Guimarães, J. R. D., Lago, G.P., dos Santos Antunes , F., Pais da Silva, M.I. “Effect of ethanol on the biodegradation of gasoline in an unsaturated tropical soil” International Biodeterioration & Biodegradation 2009, vol. 63, pp. 208–216

Pontedeiro, E.M., Simunek, J., Cotta, R.M., van Genuchten, M. Th. “The effects of preferential flow and soil texture on risk assessments of a NORM waste disposal site” Journal of Hazardous Materials, 2010, vol. 174, pp. 648–655.

Poulsen, M., Lemon, L., Barker, J.F. “Dissolution of Monoaromatic hydrocarbons into groundwater from gasoline oxygenate mixtures.” Environ Sci Technol. 1992 vol. 26(12), pp. 2483–2489.

Powers, S.E., Corseuil, H.X., Hunt, C.S., Heermann, S.E., Rice, D., Alvarez, P.J.J. “The transport and fate of ethanol and BTEX in groundwater contaminated by gasohol” Critical reviews in science and technology, 2001, vol. 31(1), pp. 79-131

Rixey, W.G. 1994. “The effect of oxygenated fuels on the mobility of gasoline components in groundwater.” *Proceedings* of the Petroleum Hydrocarbons and Organic Chemicals in Groundwater: Prevention, Detection, and Remediation. National Ground Water Association, Dublin,OH, pp. 75-90.

Rixey, W.G., He, X., Stafford, B.P. “The impact of gasohol and fuel-grade ethanol on BTX and other hydrocarbons in ground water: Effect on concentrations near a source.” American Petroleum Institute Technical Publication, 2005, vol. 23.

Schaap, M.G., Leij, F.J. “Database Related Accuracy and Uncertainty of Pedotransfer Functions.” Soil Science, 1998, vol. 163 pp. 765-779.

Schaap, M.G., F.J. Leij, van Genuchten M. Th. “Rosetta: a computer program for estimating soil hydraulic parameters with hierarchical pedotransfer functions.” Journal of Hydrology, 2001, vol. 2511 pp. 63-176.

Schneider, A.C., Corseuil, H.X. “Ethanol migration in the unsaturated zone: Real time analyses in a controlled release field experiment”. Water research, june 2012.

Schneider, A.C. “Estudo em tempo real da migração de etanol na zona vadosa em experimento de campo” MsC Thesis, April 2012

Silliman, S.E., Berkowitz, B., Simunek, J., van Genuchten, M. Th. “Fluid Flow and Solid Migration Within the Capillary Fringe.” Ground Water, 2002, vol. 40(1), pp.76-84

Simunek, J., Sejna, M., Saito, H., Sakai, M., van Genuchten, M. Th., “The HYDRUS-1D software package for simulating the one-dimensional movement of water, heat, and multiple solutes in variably-saturated media, Version 4.0, Hydrus Series 3”, Department of Environmental Sciences, University of California Riverside, Riverside, CA, USA, 2008

Spalding R.F., Toso, M.A., Exner, M.E., Hattan, G., Higgins, T.M., Sekely, A.C., Jensen, S.D. “Long-Term Groundwater Monitoring Results at Large, Sudden Denatured Ethanol Releases.” Ground Water Monitoring & Remediation, 2011, vol.31(3) pp. 69–81

Stafford, B.P. ”Impacts to groundwater from releases of fuel grade ethanol: Source behavior.” Ph.D. dissertation, Department of Civil and Environmental Engineering, University of Houston. 2007

Stafford, B.P., Rixey, W.G. “Distribution of Fuel-Grade Ethanol near a Dynamic Water Table.” Ground Water Monitoring & Remediation, 2011, vol.31(3) pp. 55-60.

Toride, N., F. J. Leij, and M. Th. van Genuchten," A comprehensive set of analytical solutions for nonequilibrium solute transport with first-order decay and zero-order production." Water Resour. Res. 1993, vol. 29(7), pp. 2167-2182.

Topp, G.C., Davis, J.L. Annan, A.P. "Electromagnetic determination of soil water content" Water Resource Res, 1980, vol 16 pp. 574-582.

Van Genuchten, M.Th. "A closed-form equation for predicting the hydraulic conductivity of unsaturated soils." Soil Sci. Am. J., 1980, vol 44 pp. 892-898.

Van Genuchten, M. Th., Parker, J.C. "Boundary conditions for displacement experiments through short laboratory soil columns". Soil Sci. Soc. Am. J. 1984, vol. 48, pp. 703-708.

Zhang, Y., Khan, I. A., Chen, X., Spalding, R.F., "Transport and degradation of ethanol in groundwater". Journal of Contaminant Hydrology, 2006, vol. 82, pp.183– 194.

Annex 1: GPR data E85 experimental area

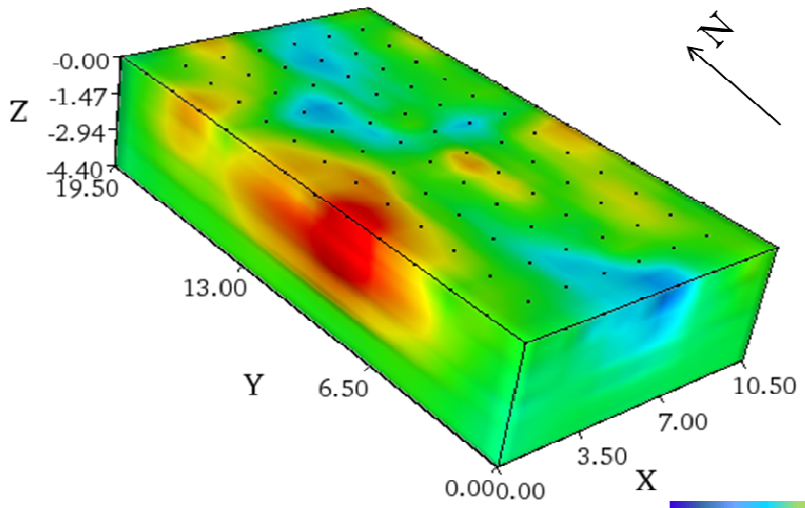

3D image of the E85 experimental area

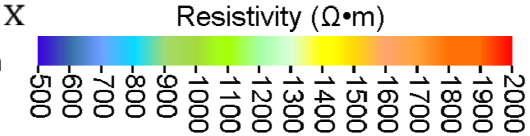

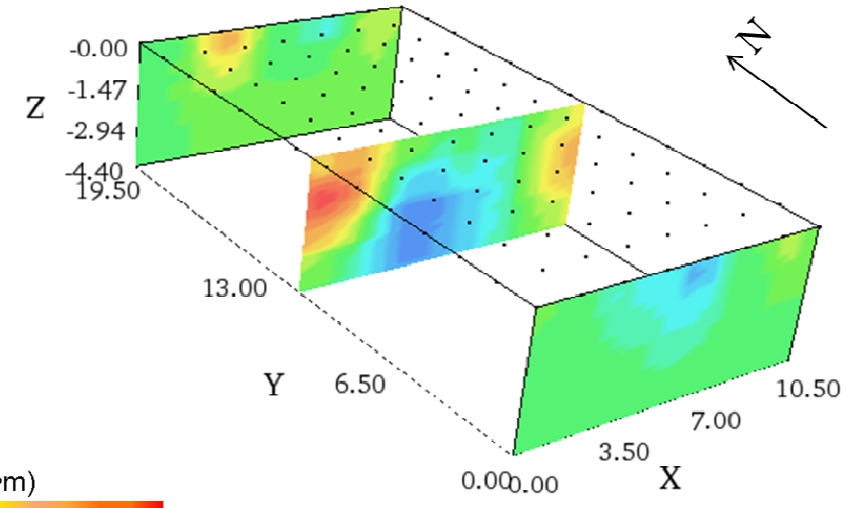

XZ planes of the E85 experimental area

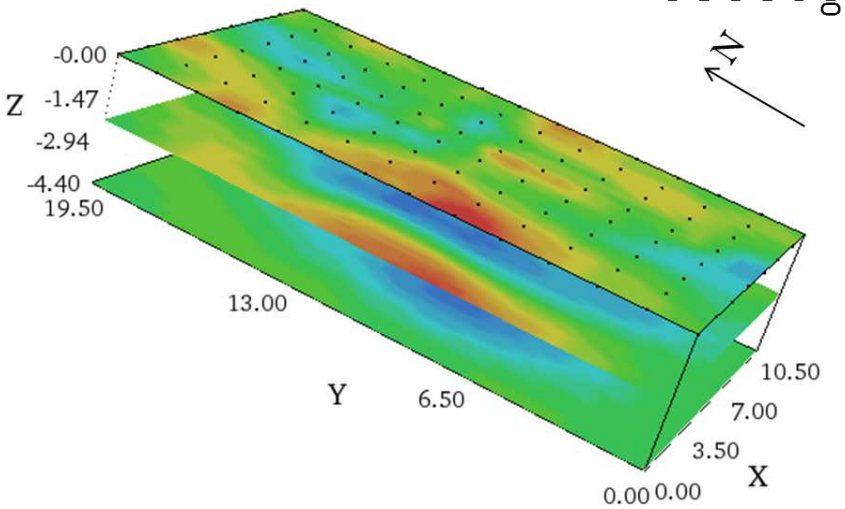

XY planes of the E85 experimental area

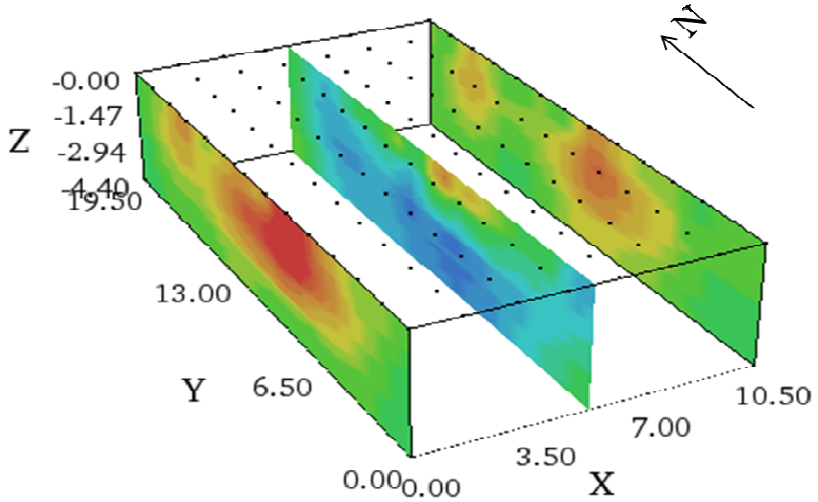

YZ planes of the E85 experimental area